Journal of the Geological Society

https://doi.org/10.1144/jgs2020-263 | Vol. 179 | 2022 | jgs2020-263

Unconformity development in retroarc foreland basins: implications for the geodynamics of Andean-type margins



Brian K. Horton

Institute for Geophysics and Department of Geological Sciences, Jackson School of Geosciences, University of Texas at Austin, Austin, TX 78712, USA

BKH, 0000-0002-1402-3524

Correspondence: horton@jsg.utexas.edu

Abstract: Unconformities in foreland basins may be generated by tectonic processes that operate in the basin, the adjacent fold—thrust belt or the broader convergent margin. Foreland basin unconformities represent shifts from high accommodation to non-depositional or erosional conditions in which the interruption of subsidence precludes the net accumulation of sediment. This study explores the genesis of long-duration unconformities (>1–20 myr) and condensed stratigraphic sections by considering modern and ancient examples from the Andes of western South America. These case studies highlight the potential geodynamic mechanisms of accommodation reduction and hiatus development in Andean-type retroarc foreland settings, including: (1) shortening-induced uplift in the frontal thrust belt and proximal foreland; (2) the growth and advance of a broad, low-relief flexural forebulge; (3) the uplift of intraforeland basement blocks; (4) tectonic quiescence with regional isostatic rebound; (5) the end of thrust loading and flexural subsidence during oblique convergence; (6) diminished accommodation or sediment supply due to changes in sea-level, climate, erosion or transport; (7) basinwide uplift during flat-slab subduction; and (8) dynamic uplift associated with slab window formation, slab break-off, elevated intraplate (in-plane) stress, or related mantle process. These contrasting mechanisms can be distinguished on the basis of the spatial distribution, structural context, stratigraphic position, palaeoenvironmental conditions, and duration of unconformities and condensed sections.

Thematic collection: This article is part of the Fold-and-thrust belts collection available at: https://www.lyellcollection.org/cc/fold-and-thrust-belts

Received 31 December 2020; revised 30 September 2021; accepted 12 October 2021

Unconformities in foreland basins can be attributed to tectonic, climatic, eustatic and internally driven (autogenic) processes. These forcing mechanisms determine zones of erosion, deposition, sediment bypass, sediment starvation and stratigraphic condensation in the fold–thrust belt, foreland basin and adjacent craton (Fig. 1). This paper considers long-duration (>1–20 myr) unconformities and condensed stratigraphic intervals in foreland settings, explores potential modes of hiatus development and evaluates the geodynamic processes affiliated with modern and ancient examples from the Andes and its retroarc foreland basin system.

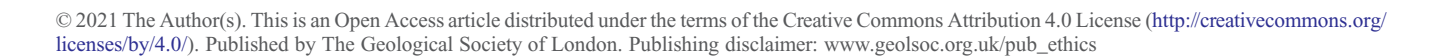
For the purpose of this study, an unconformity is defined as a 3D (planar or non-planar) surface representative of a substantial temporal hiatus resulting from non-deposition or erosion. A condensed section (or zone of stratigraphic condensation) is defined as a concordant stratigraphic interval of limited thickness (generally <5–100 m) produced by slow sediment accumulation with possible intermittent non-deposition and/or minor erosion. Unconformities and condensed sections may form stratigraphic discontinuities between diverse facies in marine or non-marine depositional systems, and may be confined to proximal or distal basin margins or may occur as basinwide features (e.g. Blackwelder 1909; Barrell 1917; Wheeler 1958; Vail *et al.* 1984; Loutit *et al.* 1988; Shanmugam 1988; Clari *et al.* 1995; Miall 2016).

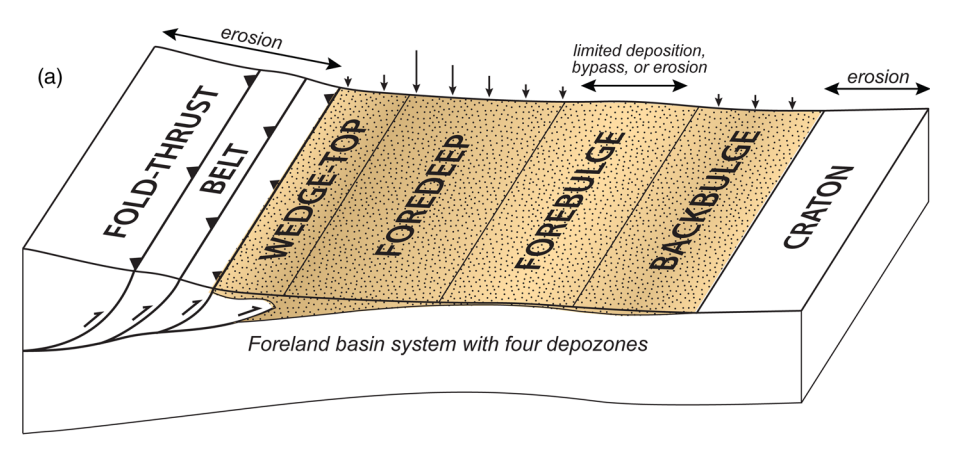
The foreland unconformities and condensed intervals discussed here span >1-20 myr and may be diachronous (time-transgressive). In other systems, the terms paraconformity or diastem may be suitable for a disconformity (non-angular unconformity) or condensed section of shorter duration. To avoid the confusion that may accompany the interpretation of unconformities – such as the debate over the genesis of the first unconformity identified by James

Hutton (e.g. Tomkeieff 1962; Young and Caldwell 2009; Jutras *et al.* 2011) – this study attempts to delineate the specific temporal and spatial framework for the reported stratigraphic discontinuities. For simplicity, the term hiatus (rather than lacuna or vacuity; Wheeler 1958) is used to refer to the period of time demarcated by a particular unconformity or condensed interval.

Foreland basins develop in contractional orogenic systems along convergent plate boundaries, in peripheral and pro-wedge/retrowedge settings within continental collision zones and in retroarc settings associated with Andean-type subduction margins. Foreland basins record long-term (>10-100 myr) rapid sediment accommodation, principally in response to regional isostatic (flexural) subsidence due to thrust loading and crustal thickening in the adjacent orogenic wedges (Price 1973; Dickinson 1974; Beaumont 1981; Jordan 1981). Foreland basins are also affected by far-field dynamic processes resulting from mantle flow and mechanical coupling between the subducting/underthrusting slab and the overriding plate (Royden 1993; DeCelles and Giles 1996; Liu et al. 2011). Most foreland basins can be categorized into two endmember geometries (Jordan 1995; Sinclair 1997; DeCelles 2012): (1) an 'overfilled' basin commonly composed of aggradational wedge-top, foredeep, forebulge and backbulge depozones (Fig. 1a); or (2) an 'underfilled' basin defined by a single aggradational foredeep depozone bordered distally by a degradational forebulge and craton (Fig. 1b).

Foreland basin unconformities are most readily formed near the erosive basin margins, along both the distal cratonic margin and the structurally disrupted proximal basin margin adjacent to the bounding fold–thrust belt (Fig. 1). Given the long-term cratonward advance of orogenic wedges and genetically linked foreland basins (Bally *et al.* 1966; Dewey and Bird 1970; Coney 1973), these basin





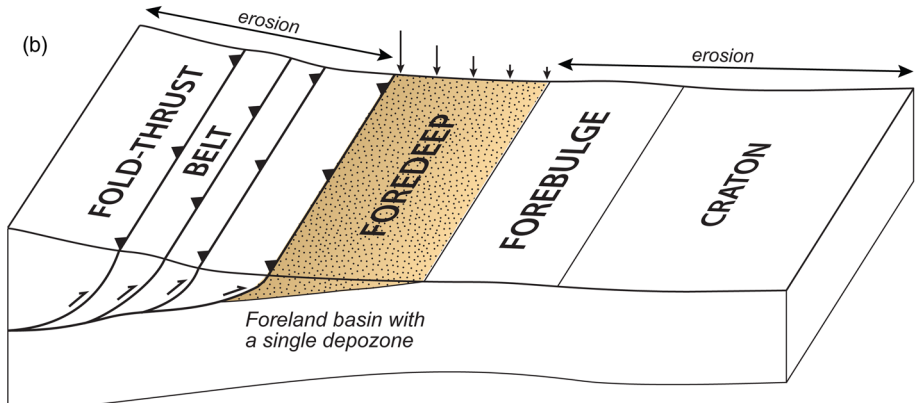


Fig. 1. Schematic block diagrams showing the principal zones of deposition and erosion within (a) a complete (overfilled) four-component foreland basin system consisting of wedge-top, foredeep, forebulge and backbulge depozones and (b) an underfilled foreland basin with a single foredeep depozone. Erosion is focused in the flanking thrust belt and craton regions, with potential erosion, sediment bypass or severely limited sediment accumulation across the forebulge region. The relative magnitude of sediment accommodation is denoted by spatial variations in basin-fill thickness (stippled pattern) and flexural subsidence (vertical arrows).

margin unconformities are preferentially concentrated in the lower and upper stratigraphic levels of foreland basin successions (Fig. 2).

In lowermost stratigraphic levels, a basal foreland unconformity may denote a basinwide stratigraphic boundary between preorogenic deposits below and synorogenic deposits above. The progressive advance of the thrust-induced flexural load and corresponding foreland subsidence profile (i.e. the flexural wave) generates a diachronous (time-transgressive) hiatus marked by this regional basal contact in which the overlying synorogenic deposits onlap the exposed distal basin margin and become progressively younger toward the craton (Fig. 2) (Cant and Stockmal 1989; Sinclair et al. 1991; Crampton and Allen 1995; DeCelles and Giles 1996; Gupta and Allen 2000). An additional basinward younging pattern is recorded in overfilled foreland basins, where a diachronous condensed interval or disconformity symbolizes the cratonward advance of the forebulge (Fig. 2a). In upper stratigraphic levels, local unconformities expressed in the proximal foreland basin register shortening and erosion in the frontal sector of the orogenic wedge. Such wedge-top deposits are distinguished by angular unconformities and growth stratal geometries produced during coarse sediment accumulation in proximity to active fold-thrust structures (e.g. Riba 1976; Anadón et al. 1986; Suppe et al. 1992; Jordan et al. 1993; Horton and DeCelles 1997; Ghiglione et al. 2010).

Idealized chronostratigraphic cross-sections or Wheeler diagrams (Wheeler 1958; Miall 2016) highlight the long-term diachronous record of foreland depozones, unconformities and condensed stratigraphic intervals (Fig. 2). In overfilled basin systems (Figs 1a and 2a), a fully developed vertical stratigraphic succession (as per Walther's law) consists of a basal foreland unconformity overlain successively by distal backbulge deposits, a condensed interval (zone of stratigraphic condensation) or a disconformity marking the forebulge, a thick upward-coarsening foredeep section and capping wedge-top deposits with growth strata and structurally controlled discordances. By contrast, underfilled basins (Figs 1b and 2b) are characterized by a basal angular or non-angular unconformity,

which represents protracted erosion across the distal forebulge and craton, overlain by a thick continuous foredeep succession.

Although these end-member cases provide useful templates, they fail to capture the complexity of foreland basins with unconformities that are not confined to the proximal and distal basin margins. This paper explores possible mechanisms for the regional generation of long-duration stratigraphic discontinuities within retroarc foreland basins, with implications for the geodynamics of Andean-type convergent plate boundaries. The motivation is to describe these possibilities and critically assess ancient and modern examples from the Andean foreland basin of western South America. Whereas others have focused on the stratigraphic records of hinterland deformation (e.g. Steinmann 1929; Mégard et al. 1984; Noblet et al. 1996; Horton 2012), the neotectonics of the modern foreland (e.g. Proyecto Multinacional Andino 2009; Veloza et al. 2012; Folguera et al. 2015a; Costa et al. 2020) or the longterm evolution of the foreland basin system (e.g. Jordan and Alonso 1987; Cooper et al. 1995; Jordan et al. 2001a; DeCelles and Horton 2003; Gómez et al. 2005; Bayona et al. 2008, 2020; Horton et al. 2010, 2020; Roddaz et al. 2010; Horton 2018a, b), this study highlights the Andean-type geodynamic processes capable of producing foreland stratigraphic hiatuses of considerable duration and spatial extent.

Mechanisms of unconformity development

Summarized here are potential unconformity generation mechanisms for retroarc foreland basins (Fig. 3). Each is distinct, but they are not mutually exclusive; several different processes may affect a single region and may operate in synchroneity or in temporal succession. The separate options are unified in that each serves to interrupt an otherwise continuous process of rapid sedimentation and accommodation generation (Figs 1 and 2). Of the eight mechanisms discussed, the first three (Fig. 3a–c) create unconformities or condensed stratigraphic intervals in relationship to specific

Unconformities and geodynamics of foreland basins

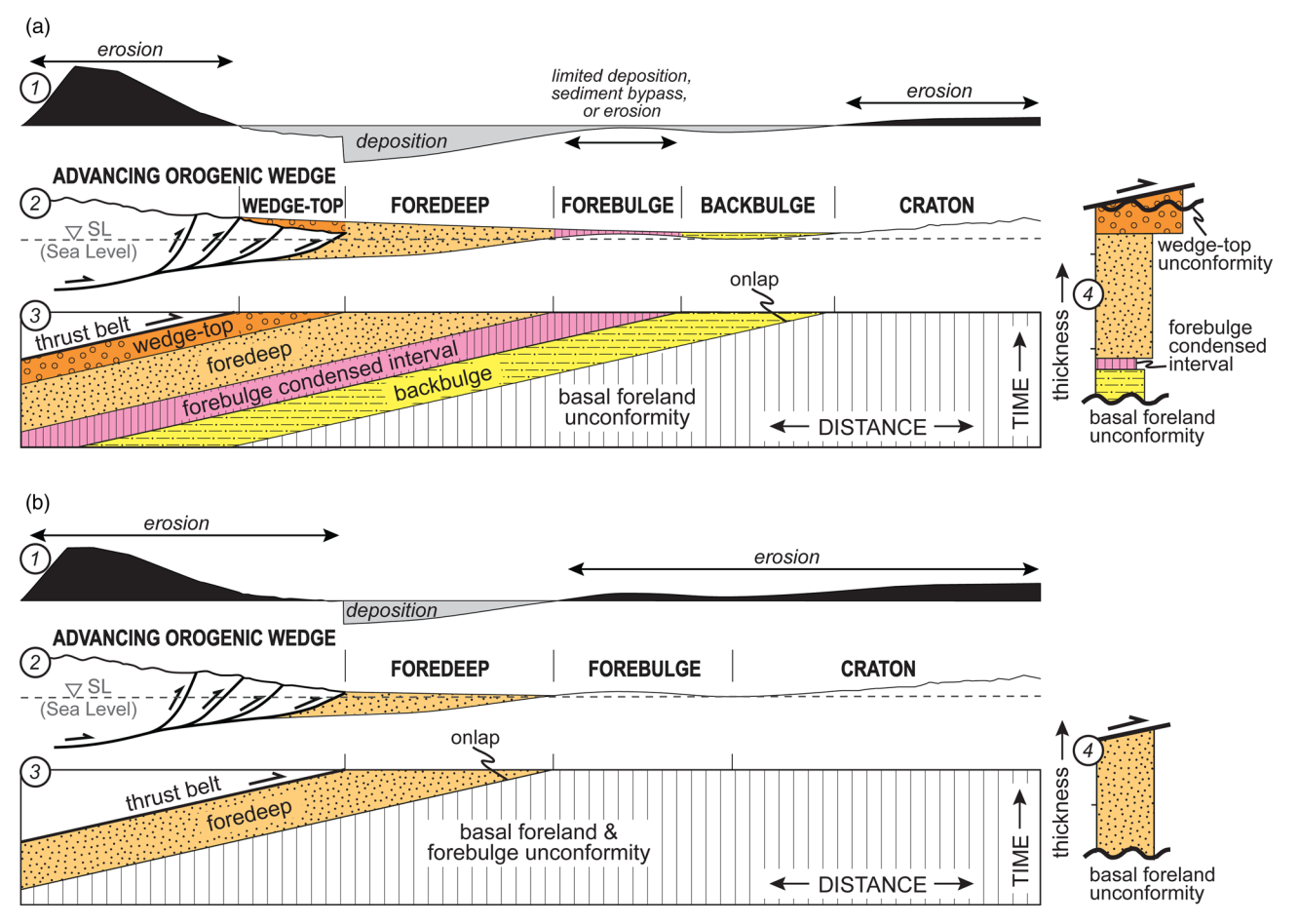


Fig. 2. Idealized diagrams for (a) a complete (overfilled) foreland basin system (Fig. 1a) and (b) an underfilled foreland basin (Fig. 1b) showing (1) the erosion/deposition profile along (2) a regional cross-section (with foreland basin subsidence profile) spanning the thrust belt to craton, with the long-term basin evolution represented by (3) an idealized time-stratigraphic cross-section (Wheeler diagram) and (4) the corresponding schematic stratigraphic succession. Progressive cratonward advance of the orogenic belt and foreland basin (i.e. the flexural wave) results in time-stratigraphic charts showing diachronous (time-transgressive) stratigraphic boundaries (between the deposits of adjacent depozones) and depositional onlap toward the craton (with an increase in hiatus duration toward the craton). Hiatuses (vertical ruled pattern) in the time-stratigraphic charts represent disconformities (non-angular unconformities) and condensed intervals in the stratigraphic record. The upward-coarsening foreland stratigraphic succession reflects successive vertical stacking of laterally adjacent, distal to proximal depozones (per Walther's law) during orogenic advance.

structures or broad structural highs, whereas the others (Fig. 3d–h) involve regional geodynamic processes that may affect large expanses of the foreland basin and its margins. The proposed mechanisms have been identified in previous syntheses and some may apply to non-foreland settings (e.g. Vail *et al.* 1984; Weimer 1984; Loutit *et al.* 1988; Shanmugam 1988; Ettensohn 1994; Crampton and Allen 1995; DeCelles 2012; Miall 2016; George *et al.* 2020).

Unconformities and condensed sections may occur throughout a foreland basin succession and need not be restricted to specific stratigraphic levels. This paper considers long-duration discontinuities that span >1-20 myr. In practice, insufficient age control will pose challenges to the precise quantification of hiatuses. In particular, condensed intervals - where several metres of section represent long periods of time - may contain a series of internal surfaces formed by multiple phases of abandonment or erosion, with the common presence of non-marine pedogenic facies or gravel lag deposits. The following mechanisms (Fig. 3) are regarded as viable explanations for lengthy hiatuses that may be embodied in the stratigraphic record as: (1) an unconformity defined by a single erosive or non-erosive surface; (2) an unconformity capped by thin regolith or gravel lag deposits; or (3) a condensed section potentially rich in palaeosols or other facies indicative of reduced accommodation.

Shortening in the frontal thrust belt and proximal foreland

Uplift in the frontal fold-thrust belt can produce unconformities in the proximal, wedge-top sector of a foreland basin (Fig. 3a). Progressive syndepositional tilting of basin fill results in growth strata recognized by an up-section decrease in dip, abrupt lateral thickness variations (thinning onto the synchronous fold-thrust structure) and internal angular unconformities (Birot 1937; Riba 1976; Anadón et al. 1986; Suppe et al. 1992). The spatial extent of a wedge-top unconformity and growth stratal package is governed by the wavelength of the adjacent structure and is therefore limited to a short horizontal distance (typically <5–10 km) from the syndepositional thrust fault and related fold (e.g. DeCelles 1994; Ghiglione et al. 2002; Perez and Horton 2014). This constraint on the thrust front position through time provides crucial insights for the reconstruction of thrust belt development (e.g. Jordan et al. 1993, 2001a; DeCelles and Giles 1996; DeCelles and Horton 2003; Ghiglione and Ramos 2005; DeCelles et al. 2011).

The proximity to active structures ensures that wedge-top unconformities and associated growth strata in clastic systems are confined to coarse facies near the mountain front (Figs 1 and 2a). Given this restricted spatial extent, any proximal stratigraphic discordances are expected to pass rapidly into correlative conformable sections in the laterally adjacent foredeep (Fig. 3a).

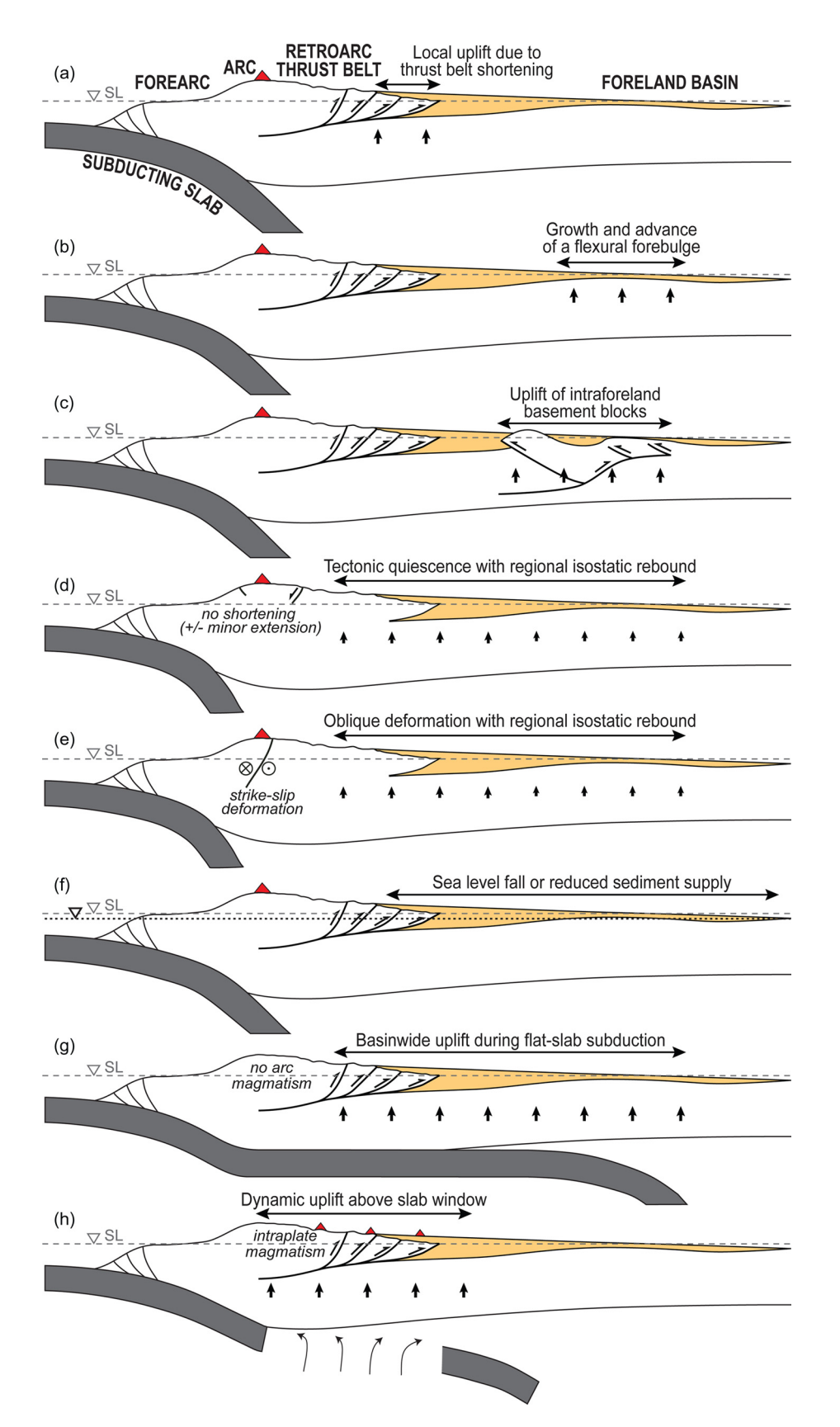


Fig. 3. Schematic cross-sections showing potential geodynamic mechanisms for the generation of unconformities and condensed stratigraphic intervals in a foreland basin, including: (a) localized shortening-related uplift in the frontal thrust belt and proximal foreland; (b) growth and advance of a broad, low-relief flexural forebulge in the distal foreland; (c) uplift of intraforeland basement blocks along crustal-scale reverse faults; (d) tectonic quiescence with regional isostatic rebound; (e) cessation of thrust loading and flexural subsidence during oblique convergence; (f) diminished accommodation or sediment supply due to changes in sea-level, climate, erosion or sediment transport; (g) basinwide uplift caused by increased interplate coupling during flat-slab subduction; and (h) dynamic uplift associated with slab window formation, slab break-off, elevated intraplate (in-plane) stress or related mantle processes.

Growth and advance of a broad, low-relief flexural forebulge

An advancing orogenic wedge may yield a widespread unconformity that denotes a diachronous hiatus induced by the cratonward migration of the flexural wave during progressive topographic loading (Figs 2 and 3b). This long-term process may be manifest not only as a basal foreland unconformity separating pre-orogenic from

synorogenic deposits (e.g. Sinclair *et al.* 1991; Crampton and Allen 1995; Caballero *et al.* 2020), but also as a discrete condensed interval or disconformity indicative of an advancing broadwavelength, low-amplitude forebulge (Fig. 2a) (Plint *et al.* 1993; DeCelles and Horton 2003; Fuentes *et al.* 2009; DeCelles 2012). The continuous advance of a flexural forebulge at a fixed rate is considered unlikely. Unsteady processes involving irregular advances or punctuated 'jumps' in forebulge location are deemed

more probable due to the preferential reactivation of pre-existing structures, stratigraphic anisotropies or inherited basement fabrics (Waschbusch and Royden 1992a; Bayona and Thomas 2003, 2006; DeCelles 2012; Chapman and DeCelles 2015). Moreover, spatial variations in plate strength will influence forebulge migration, with a stronger plate (i.e. higher flexural rigidity and effective elastic thickness) toward the craton fostering a greater flexural wavelength and broader forebulge through time (e.g. Stockmal *et al.* 1986; Waschbusch and Royden 1992*b*; Fosdick *et al.* 2014).

The regional basin architecture in terms of underfilled/overfilled geometry (Jordan 1995) and the site-specific geomorphic and palaeoenvironmental conditions – most crucially, the local ratio of accommodation to sediment supply (Horton 2018a) – will determine whether the broad, low-relief forebulge will involve (1) erosion, (2) sediment bypass or (3) modest sediment accumulation and, in turn, result in, respectively, (1) an unconformity defined by a single erosional surface, (2) an unconformity potentially marked by relict detritus in the form of a thin gravel lag or (3) a condensed depositional interval routinely demarcated in non-marine clastic systems by pedogenic facies. Preservation of the predicted forebulge stratigraphic record within an overfilled four-component basin system (Figs 1a, 2a and 3b) requires considerable lateral mobility of the fold-thrust belt and therefore will be limited to orogenic systems with largemagnitude shortening and crustal thickening (e.g. DeCelles and DeCelles 2001; Christophoul et al. 2003; DeCelles 2012).

Uplift of intraforeland basement blocks

Intraforeland basement block uplifts disconnected from the thinskinned fold-thrust belt can produce unconformities and condensed intervals over large swaths of a foreland basin (Fig. 3c). Because many intraforeland uplifts are formed by independent structures deeply rooted in the lower crust, the spatial scale of associated stratigraphic discontinuities can be large (i.e. several tens of kilometres) (e.g. Tweto 1980; McQueen and Beaumont 1989; Erslev 2005; Rudolph et al. 2015; Folguera et al. 2015c). The interplay between the relative rates of rock uplift, regional flexural subsidence and sediment supply will dictate whether an individual block will be emergent and build positive topography or will remain buried beneath foreland basin fill (e.g. Dickinson et al. 1988; Ramos et al. 2002; Yonkee and Weil 2015; Lawton 2019). Specifically, an isolated non-emergent block would be represented by a buried structural high that recorded diminished subsidence relative to the adjacent proximal and distal sectors of the foreland basin (Fig. 3c). By contrast, an emergent block that was later buried would prompt an erosional unconformity with a spatial distribution matching the dimensions of the block uplift. However, a block that remained a positive topographic feature for an extended period and never returned to a net accumulation situation would leave no preserved basin-fill record.

Sufficient subsurface control can enable the identification of both emergent and non-emergent basement block uplifts within a single foreland basin (e.g. Balkwill *et al.* 1995; Lalami *et al.* 2020). Although a basement block uplift in the distal foreland may be difficult to distinguish from a flexural forebulge (e.g. Ziegler *et al.* 2002), most intraforeland block uplifts exhibit a lower wavelength (width), a higher structural relief and can be geometrically linked to crustal-scale structures of moderate to large displacement (several to tens of kilometres) (Fig. 3c) (e.g. Bayona and Thomas 2003, 2006).

Tectonic quiescence with regional isostatic rebound

A prolonged pause in crustal shortening and flexural loading may promote isostatic rebound and the development of an unconformity across the foreland basin (Fig. 3d). During a period of tectonic quiescence, continued erosion would decrease the orogenic topography, causing flexural unloading and minor isostatic uplift that would diminish in magnitude toward the craton. This process would yield an unconformity characterized by erosion in the proximal foreland and sediment bypass or severely reduced accommodation in the medial to distal foreland (e.g. Heller *et al.* 1988; Cant and Stockmal 1989; Legarreta and Uliana 1991; Ross *et al.* 2005; Morin *et al.* 2019).

Alternating short-term phases of thrust fault activity and quiescence have been invoked to explain foreland hiatuses (Flemings and Jordan 1990; Miall 1996; Catuneanu *et al.* 1997; Houston *et al.* 2000; Londono *et al.* 2012). Such episodic thrusting appears intuitively appealing because the seismogenic records of individual faults define cyclical patterns over periods <10 kyr (Avouac 2003; Allmendinger *et al.* 2009). However, over longer time frames (>1 myr), thrust faults and kinematically linked fold-thrust systems show sustained shortening without evidence of orogen-wide episodicity (Jordan *et al.* 1993, 2001*a*; Beaumont *et al.* 2000; Allmendinger and Judge 2014; Mouthereau *et al.* 2014; Anderson *et al.* 2018). Therefore, long pauses in regional shortening are not an intrinsic or autogenic component of contractional orogenic belts and require specific mechanisms of sufficient duration.

Rather than autogenic behaviour, long-term (>1 myr) cessation of shortening in a fold—thrust belt may be the expression of persistent tectonic quiescence due to lowered convergence rates and/or a shift to a neutral or modestly tensile stress regime (Fig. 3d). Commonly, these drivers may be genetically related to slab rollback (retrograde slab motion) during steepening of the subducting/ underthrusting slab, potentially within a retreating plate boundary involving reduced mechanical interplate coupling between the converging plates (e.g. Dewey 1980; Royden 1993; Barberón *et al.* 2018; Horton 2018*b*; Fernández Paz *et al.* 2019).

Cessation of thrust loading and flexural subsidence during oblique convergence

A foreland basin unconformity may be generated by the termination of flexural subsidence during a shift from a contractional to largely strikeslip tectonic regime (Fig. 3e). The obliquity of plate convergence is an important control on the amount of strike-slip and contractional deformation in the overriding plate. Strain partitioning along a convergent margin during non-orthogonal plate motion (Fitch 1972; Jarrard 1986) is likely to regulate the relative proportions of strike-slip displacement and crustal thickening within the orogenic system, including structures in the forearc, magmatic arc and retroarc fold—thrust belt. A shift to highly oblique convergence has been recognized as a trigger for the termination of orogenic thickening, crustal loading and flexural subsidence in an adjacent foreland (e.g. Price 1994; Jaillard and Soler 1996; Simony and Carr 2011).

Although similar to the preceding option of a regional stratigraphic hiatus related to erosional unloading and minor flexural rebound (Fig. 3d), the distinction in this case (Fig. 3e) is that the convergent margin experiences not only a lessening in the rates of orthogonal (trench-normal) convergence, but also an increase in strike-slip deformation. Ultimately, the consequences within the foreland basin are similar, with the establishment of an extensive erosional unconformity that diminishes in magnitude toward the craton. A potential alternative is that an inboard jump in strike-slip deformation may compartmentalize the foreland basin into a series of smaller strike-slip basins (e.g. de Vicente *et al.* 2011).

Diminished accommodation or sediment supply due to changes in sea-level, climate, erosion or transport

A large decline in either accommodation or sediment supply may induce an unconformity across a foreland basin (Fig. 3f). Under appropriate conditions, a fall in relative sea-level could effectively

eliminate sediment accommodation across the basin. Basinwide erosion will only occur if the magnitude of the drop in regional base level is sufficiently large to exceed accommodation generation by flexural and dynamic mechanisms (Vail *et al.* 1984; Shanmugam 1988; Jordan and Flemings 1991; Dickinson *et al.* 1994; Clevis *et al.* 2004). In such situations, given the low topographic gradients across most foreland basins, the magnitude of erosion should be relatively uniform across the width of the basin (Fig. 3f). The resulting stratigraphic record is apt to be distinguished by widespread incision, with cutting of incised valleys several tens to possibly 100–200 m deep (e.g. Weimer 1984; Van Wagoner 1995; Plint *et al.* 2012).

Alternatively, in the absence of a base level change, the same effects could be accomplished by modifications in climate or erosional intensity that affect sediment supply, transport capacity and stream power. As examples, long phases of non-deposition, sediment bypass or erosion may be the respective outcomes of: (1) a sharply reduced sediment supply due to aridification or minimized weathering; (2) a shift to highly efficient sediment transport across the basin; or (3) intensified erosion that leads to the evacuation of foreland basin fill (e.g. Blisniuk *et al.* 2005; Clift 2010; Clift and Van Laningham 2010; Allen *et al.* 2013).

For orogenic wedges governed by critical taper mechanics (Dahlen and Suppe 1988), changes in climate and erosion can further regulate mass influx and outflux for the orogen and adjacent foreland, with potential shifts in the loci of crustal shortening and exhumation. Such orogenic self-organization would interact with internal (autogenic) and external agents affecting erosional/depositional mass budgets and basin sedimentation (Flemings and Jordan 1989; DeCelles and Mitra 1995; Horton 1999; Sobel *et al.* 2003; Sinclair and Naylor 2012; Ghiglione *et al.* 2019).

Basinwide uplift during flat-slab subduction

Basinwide uplift in retroarc regions may arise from the mechanical effects of a shift from normal or steep-angle subduction to flat-slab subduction (Fig. 3g). With greater compression, end-loading and/or basal traction in the overriding plate (Bird 1984; Axen et al. 2018), an accompanying reversal from subsidence to uplift in the foreland basin would eliminate accommodation and instigate pervasive erosion. This shift would be manifest as a regional erosional unconformity spanning the interval of flat-slab conditions, with a potentially younging trend toward the craton (reflecting the inboard advance of the subducted slab at depth). However, the geodynamic responses to subduction shallowing are complex and it is recognized that the precise effects of flat-slab subduction are varied and often unclear, with some studies proposing increased subsidence rather than uplift (e.g. Mitrovica et al. 1989; Liu et al. 2011; Flament et al. 2015; Gianni et al. 2018; Carrapa et al. 2019; Dávila et al. 2019; Saylor et al. 2020).

In the simplified model shown here (Fig. 3g), flat-slab subduction is considered to be responsible for increased mechanical coupling between the converging plates and the enhanced inboard transmission of compressional stress. However, similar effects across the foreland basin could be activated by long-distance material transport via crustal underthrusting, lower crustal flow, ductile injection or crustal translation above a deep décollement (e.g. Oldow *et al.* 1989; McQuarrie and Chase 2000; Erslev 2005). The broad wavelength of these processes suggests that they would not cause sharp angular discordances, but would lead to widespread exhumation of foreland basin fill.

Dynamic uplift associated with slab window formation, slab break-off or elevated intraplate stress

Dynamic uplift unrelated to thrust belt shortening and flexural loading may involve several potential geodynamic mechanisms for the origination of regional unconformities spanning foreland basins.

The formation of a slab window during the subduction of an actively spreading oceanic ridge can drive uplift of continental lithosphere above an expanding gap in the subducted slab (Fig. 3h) (Thorkelson 1996). Similarly, the tearing or break-off of a subducted slab may catalyse surface rebound and pronounced basinwide uplift (Davies and von Blanckenburg 1995; Andeweg and Cloetingh 1998; Gianni *et al.* 2018, 2019). Slab window formation, slab tearing and slab break-off promote uplift by way of heating and/or asthenospheric upwelling (Fig. 3h). These have a profound effect on magmatism, provoking a switch from subduction-related continental arc magmatism to anomalous intraplate (within-plate) magmatism with strong mantle/asthenospheric signatures.

At similar scales, the possible far-field transmission of intraplate (in-plane) compressional stress from a plate boundary may induce large-wavelength lithospheric folding or buckling (Ziegler *et al.* 2002; Kley and Voigt 2008; Cloetingh and Burov 2011; Lacombe and Bellahsen 2016). Alternatively, vertical motion associated with plume activity or mantle flow may yield broadly similar uplift patterns in the absence of elevated horizontal compressional stress (Burov and Cloetingh 2009; Faccenna and Becker 2020).

The aforementioned geodynamic mechanisms mostly reflect dynamic processes linked to subduction, plate interactions, mechanical coupling and/or mantle flow that result in large-scale basin abandonment and the creation of stratigraphic hiatuses. These factors could arrest foreland subsidence, prompt erosion across the basin and generate a regional disconformity.

Case studies from the Andean foreland basin

Geodynamic mechanisms of unconformity development are assessed for six examples from the Andean retroarc foreland basin (Fig. 4): three examples involving lower to mid-Cenozoic foreland basin fill, now uplifted in the Andean fold–thrust belt, and three examples from the Pliocene–Quaternary record of the modern foreland basin. These separate cases are unified by stratigraphic records with long-duration hiatuses (Fig. 5) that demonstrate the interruption of otherwise continuous accommodation generation.

The six situations span different time frames, deformation scenarios, climatic settings and geodynamic configurations. These include: (1) regions with the greatest shortening, thickest crust and highest mean elevation (in the central Andes of southern Peru, Bolivia and northern Argentina); (2) zones of low shortening, normal crustal thickness and subdued orogenic topography (the southern Andes, including Patagonia); and (3) areas involving the accretion of oceanic materials during transpressional reactivation of older extensional systems (the northern Andes of northern Peru, Ecuador and Colombia) (Kley et al. 1999; Aleman and Ramos 2000; Mora et al. 2010; Horton 2018b). The climatic conditions are markedly varied due to the zonal atmospheric circulation and rain shadow effects, which yield high-magnitude precipitation in retroarc sectors of the northern and central Andes, but sharply lower precipitation in the southern Andean foreland (Montgomery et al. 2001). Spatially irregular glaciation has disproportionately affected higher elevation Andean districts and large parts of the southern Andes (e.g. Bourgois et al. 2000; Ghiglione et al. 2019).

Andean plate tectonic configurations vary latitudinally (Fig. 4), as expressed in (1) restricted provinces of flat-slab subduction (e.g. the Colombian/Bucaramanga (2–8° N), Peruvian (5–15° S) and Chilean/Pampean (27–33° S) flat-slab segments), (2) the subduction of aseismic ridges (e.g. the Sandra (5–6° N), Carnegie (0–2° S), Nazca (14–16° S) and Juan Fernández (32–34° S) Ridges); and (3) the subduction of active oceanic spreading ridges and opening of asthenospheric slab windows (e.g. the Patagonian slab window adjacent to the Chile Ridge (45–48° S) along the Nazca–Antarctic plate boundary) (Jordan *et al.* 1983; Ramos 1999, 2005; Gutscher

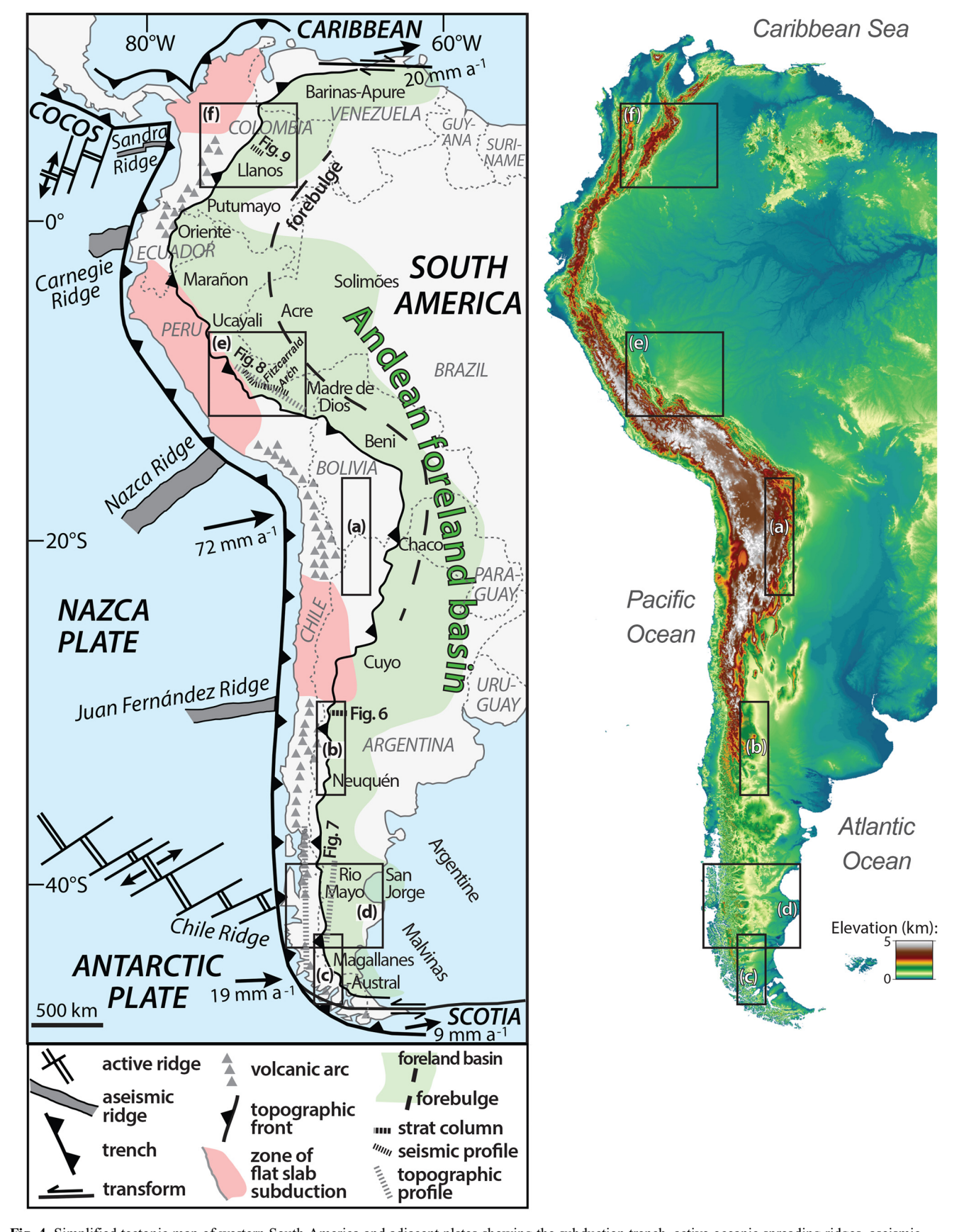


Fig. 4. Simplified tectonic map of western South America and adjacent plates showing the subduction trench, active oceanic spreading ridges, aseismic ridges, zones of flat-slab subduction, Andean magmatic arc, Andean topographic front and modern Andean foreland basin and forebulge axis (modified from Horton 2018a, b; after Ramos and Folguera 2009). Plate velocities are shown relative to the South American plate (DeMets et al. 2010). The box outlines indicate the locations of the six case studies of unconformities and condensed stratigraphic intervals within three ancient segments of the Andean foreland basin (north–south strips; Fig. 5a–c) and three modern segments of the basin (squares; Fig. 5d–f), along with representative stratigraphic, topographic and seismic profiles (Figs 6–9).

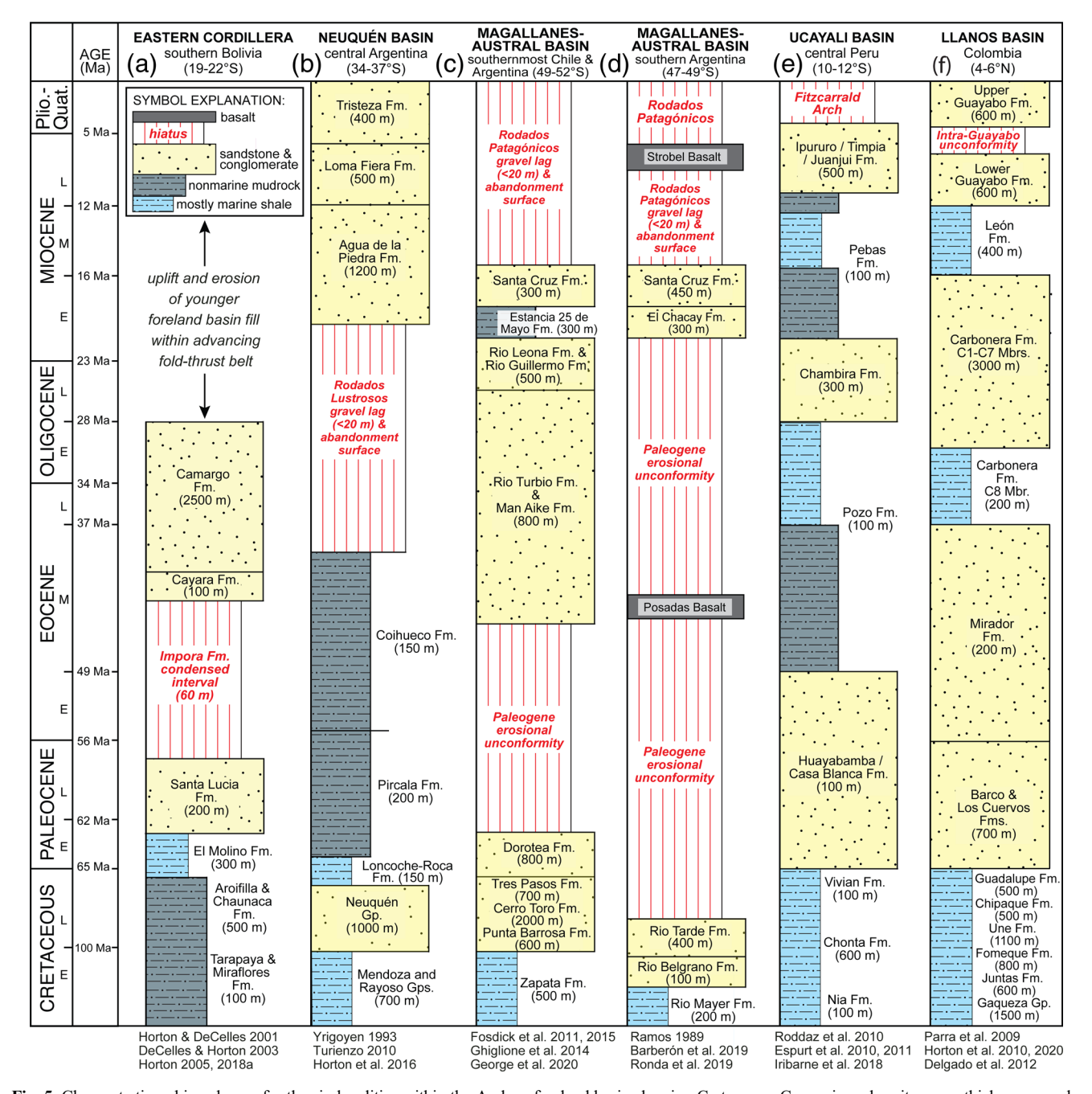


Fig. 5. Chronostratigraphic columns for the six localities within the Andean foreland basin showing Cretaceous—Cenozoic rock units, ages, thicknesses and simplified lithologies. The stratigraphic discontinuities, representing temporal hiatuses (vertical ruled pattern), are expressed in the rock record as unconformities, condensed sections or abandonment surfaces with gravel lags. Site locations are shown in Figure 4.

et al. 2000; Lagabrielle et al. 2004; Lonsdale 2005; Ramos and Folguera 2009; Wagner et al. 2017). Despite these spatial variations, modern earthquake focal mechanisms and global stress datasets show that shortening dominates most of the Andean retroarc fold—thrust belt, with low-magnitude extension restricted to elevated plateau regions and strike-slip deformation focused along the northern and southern extremities of the orogenic belt (Assumpção et al. 2016; Heidbach et al. 2018). Within the modern Andean foreland, a flexural forebulge is roughly parallel to the thrust front, consistent with a regional isostatic (flexural) response to the Andean topographic load (Horton and DeCelles 1997; Chase et al. 2009).

Current plate motions (DeMets *et al.* 2010) define nearly orthogonal Nazca–South America convergence along most of the western margin of the South American plate, excluding the northern and southern terminuses where oblique convergence and transform

motion occur at lower rates with the adjacent Caribbean, Antarctic and Scotia plates (Fig. 4). Past studies have recognized temporal variations in the relative convergence rate, absolute overriding plate velocity and convergence direction (e.g. Pilger 1984; Pardo-Casas and Molnar 1987; Somoza and Ghidella 2012). Whereas many studies have linked Andean orogenesis to Nazca–South America convergence and/or the absolute westward motion of South America (e.g. Coney and Evenchick 1994; Silver *et al.* 1998; Mpodozis and Cornejo 2012; Maloney *et al.* 2013; Horton 2018*b*), others suggest that more-oblique convergence, particularly in the early Cenozoic, may correlate with phases of diminished Andean shortening or tectonic quiescence (e.g. Jaillard and Soler 1996; Aleman and Ramos 2000; Carlotto 2013).

Six case studies from the Andean foreland basin (examples a–f) are presented individually in chronological and geographical order,

with ancient examples (examples a–c) presented from north to south (Figs 4 and 5a–c) and modern examples (examples d–f) presented from south to north (Figs 4 and 5d–f). For each locality, an overview of the chronostratigraphic relationships and description of the unconformities or condensed sections is followed by a discussion of the potential geodynamic mechanisms responsible for accommodation reduction and unconformity development.

Paleogene condensed section with palaeosols, Eastern Cordillera, southern Bolivia and northern Argentina

A widespread condensed section marked by distinctive palaeosols distinguishes the Paleogene foreland basin succession in the central Andes of Bolivia and northern Argentina (Fig. 4). The condensed stratigraphic zone (Fig. 5a) consists of a <20-100 m thick interval of stacked hypermature palaeosol horizons (or 'supersols') within the Impora Formation of Bolivia and the Maiz Gordo and Lumbrera Formations of northern Argentina (Horton and DeCelles 2001; DeCelles and Horton 2003; DeCelles et al. 2011; DeCelles 2012; Horton 2018a). These fine-grained pedogenic facies divide, with no angular discordance or erosional relief, an underlying c. 100-300 m thick Maastrichtian-Paleocene marine to distal non-marine section from an overlying Oligocene-Miocene, 2-6 km thick, upwardcoarsening succession attributed to fluvial deposition in a foredeep setting. In some locations the condensed interval is instead expressed as a single disconformity with no presence of palaeosols. Although direct age control is hindered by thorough pedogenic alteration and a lack of primary volcanic layers, age constraints from the underlying and overlying units broadly limit the condensed zone to an early/ middle Eocene to early Oligocene age (DeCelles and Horton 2003; Horton 2005; DeCelles et al. 2011; Siks and Horton 2011).

The roughly 15–20 myr condensed section (Fig. 5a) contains extremely mature palaeosols with soil horizonation (zones of leaching and accumulation, mottling, gleying and oxidation) and well-developed calcareous nodules, glaebules, peds, root traces and trace fossils, which overprint and mostly destroy the original sedimentary structures. These prominent pedogenic facies or 'supersols' are identified for up to 1000 km along strike, from 17 to 26° S (Fig. 4). The geological relationships require extremely low time-averaged rates of Paleogene sediment accumulation (<5 m/myr) over a large portion of the central Andean foreland basin, without syndepositional shortening, tilting or extensive erosion.

Potential explanations for the Paleogene condensed interval or equivalent disconformity in the central Andes at 17–26° S include: (1) climate change; (2) reduced accommodation during tectonic quiescence or oblique deformation; (3) regional uplift during flat-slab subduction; (4) intraforeland basement uplifts; and, the preferred interpretation, (5) forebulge growth and advance.

Climate change (Fig. 3f)

Elevated air temperatures and a humid climate during the Paleogene may have boosted weathering intensity and rainfall in the foreland basin (Sempere *et al.* 1997; Starck 2011), enhancing soil genesis and yielding the stacked palaeosols of the condensed section. However, such a change in climate would also have increased the supply of sediment, which is contradicted by a sharp decline in sediment accumulation during Paleogene basin evolution.

Reduced accommodation during tectonic quiescence or oblique deformation (Fig. 3d, e)

A potential Paleogene shutdown of shortening and/or transition to strike-slip deformation could explain a protracted pause in crustal loading and flexural subsidence. Although oblique Eocene deformation has been identified farther north in the hinterland districts of Peru (Carlotto 2013), a shift to strike-slip deformation is

not supported for the entire central Andean region, where subduction-related arc magmatism and retroarc shortening persisted (Mamani *et al.* 2010; Perez and Horton 2014; Horton *et al.* 2015; Garzione *et al.* 2017). For Bolivia and northern Argentina, thermochronological data indicate middle to late Eocene cooling in the hinterland, which points to erosional exhumation during sustained crustal shortening (Barnes *et al.* 2006; Gillis *et al.* 2006; Carrapa and DeCelles 2008; Rak *et al.* 2017).

Regional uplift during flat-slab subduction (Fig. 3g)

A roughly Eocene transition to shallow subduction may have promoted dynamic uplift that counteracted the effects of shortening-induced flexural subsidence. Evidence for slab shallowing derives from the time–space record of igneous activity, such that an inboard advance of arc magmatism can be attributed to the migration of the leading hinge of a shallow segment of the subducted slab (e.g. Sandeman *et al.* 1995; James and Sacks 1999; Ramos and Folguera 2011). The principal objection to this option is that dynamic uplift associated with flat-slab subduction would be unlikely to exceed the subsidence expected for thrust-generated topographic loads (see flexural models of Perez and Levine 2020).

Intraforeland basement block uplift (Fig. 3c)

Proposals for a Paleogene broken foreland basin in northern Argentina are based on local reports of minor dip discordances that are not connected to major fold—thrust structures (e.g. Montero-López et al. 2018; Payrola et al. 2020). The lack of a substantial upsection decrease in dip, the dominance of relatively fine-grained facies and the regional depositional continuity of Paleogene units (Boll and Hernández 1986; Jordan and Alonso 1987; Siks and Horton 2011; Starck 2011) preclude the large topographic barriers expected for a basin comparable with classic Laramide or Sierras Pampeanas broken foreland basins (e.g. Jordan 1995; Ramos 2009; Lawton 2019). Intraforeland uplifts also would be of insufficient scale to account for the spatial extent of the Paleogene condensed section for up to 1000 km along strike.

Forebulge growth and advance (Fig. 3b)

The favoured explanation is that diminished Paleogene sediment accumulation is the result of the growth and cratonward migration of a flexural forebulge. The accumulation of a palaeosol-rich condensed section can be ascribed to low-accommodation and lowerosion conditions across a broad-wavelength forebulge with limited relief. The large magnitude of trench-perpendicular shortening (>200–300 km), commensurate with the advance of fold-thrust deformation, and attendant crustal thickening (DeCelles and Horton 2003; McQuarrie *et al.* 2005; Uba *et al.* 2009) suggest a high lateral mobility of the foreland basin (as outlined in Fig. 2a).

The interpretation of an eastward advancing forebulge is consistent with topographic loading driven by shortening in a fold–thrust belt above a mid-crustal décollement (McQuarrie 2002). Further, the estimated 15–20 myr duration of the condensed section (Fig. 5a) is compatible with the timescales of forebulge migration expected for the reported values of Andean shortening, flexural rigidity and regional sedimentary thicknesses (e.g. Horton and DeCelles 1997; DeCelles and Horton 2003; Echavarria *et al.* 2003; McQuarrie *et al.* 2005; Anderson *et al.* 2018; Calle *et al.* 2018; Rahl *et al.* 2018).

Mid-Cenozoic hiatus, abandonment surface and gravel lag, Neuquén Basin, central Argentina

A disconformity marked by an abandonment surface and capping gravel lag demarcates a mid-Cenozoic (c. 40–20 Ma) hiatus in the

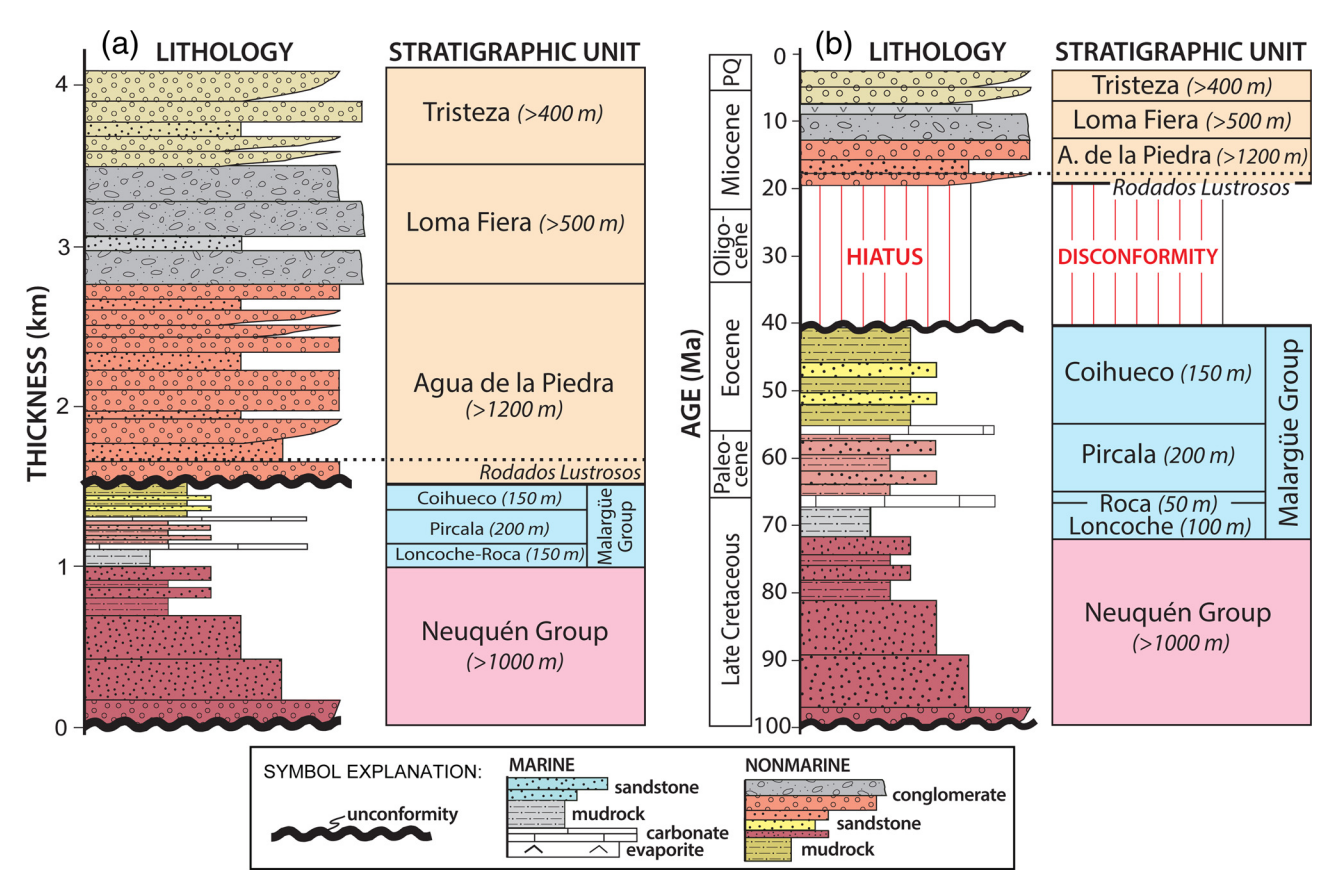


Fig. 6. Two stratigraphic columns for the northern Neuquén Basin of west-central Argentina showing (a) thickness and (b) time (age) (from Horton *et al.* 2016; Horton and Fuentes 2016). The columns show the same Upper Cretaceous–Cenozoic stratigraphic framework, including rock units, ages, thicknesses and simplified lithologies (compare with Fig. 5b). The two columns show the value of comparing stratigraphic (thickness) to time (age) depictions in assessing stratigraphic discontinuities (unconformities, condensed sections or abandonment surfaces with gravel lags) and temporal hiatuses. Site locality is shown in Figure 4.

Neuquén Basin of west-central Argentina (Fig. 4). The base of the Agua de la Piedra Formation is composed of a 2–20 m thick ultrastable conglomerate referred to as the 'Rodados Lustrosos' (Fig. 5b), which contains distinctive shiny ('lustrous') pebble and cobble clasts that are extremely smooth, well-rounded and have been polished by large-distance transport and high degrees of weathering, oxidation, recrystallization and rock varnish development (Horton et al. 2016). This diagnostic unit occurs in the middle of an Upper Cretaceous—Cenozoic foreland basin succession up to 4–5 km thick (Fig. 6). In most localities, the conglomeratic facies define a disconformable, non-angular contact with limited incision into underlying the Upper Cretaceous to middle Eocene clastic facies of the Neuquén Group and finer grained Malargüe Group (Fig. 6).

In contrast with the preceding example in the central Andes, there is no evidence of lengthy pedogenesis in the Neuquén Basin; rather, a geomorphic abandonment surface (or multiple closely spaced surfaces) is capped by a thin (<20 m) veneer of gravel. A reduction in long-term sediment accumulation and the paucity of pedogenic facies suggest that intrabasinal sediment transport from the middle Eocene to earliest Miocene resulted in bypass to distal regions to the east. A further indication of sediment bypass – as opposed to sediment starvation - includes local erosion represented by palaeovalleys in which the 'Rodados Lustrosos' unit disconformably overlies uppermost Cretaceous strata (Garrido et al. 2012). This pervasive conglomeratic unit has been identified over a >400 km distance along strike, from 33 to 37° S (Gorroño et al. 1979; Yrigoyen 1993; Sempere et al. 1994). An absolute age of c. 40-20 Ma is assigned to the hiatus (Figs 5b and 6) on the basis of maximum depositional age constraints provided by detrital zircon U-Pb geochronological results for sandstones with considerable

volcanogenic material (Horton *et al.* 2016; Horton and Fuentes 2016; Horton 2018*a*; Fuentes and Horton 2020).

Several possible options could explain the c. 20 myr mid-Cenozoic depositional hiatus in the Neuquén Basin at 33–37° S, including: (1) intraforeland basement uplifts; (2) forebulge growth and advance; (3) a change in climate or sea-level; and, the favoured interpretation, (4) reduced accommodation during tectonic quiescence.

Intraforeland basement block uplift (Fig. 3c)

The present foreland region is broken by the San Rafael uplift, a basement-involved contractional structure c. 100 km east of the modern Andean topographic front. The timing of this structure is much younger than the 40–20 Ma hiatus, with most rock uplift accomplished in the late Miocene (Ramos and Kay 2006; Ramos and Folguera 2009, 2011). No comparable mid-Cenozoic basement-involved structures of sufficient scale have been recognized at depth within the foreland basin (Boll et al. 2014).

Forebulge growth and advance (Fig. 3b)

Diminished accumulation may be the product of forebulge advance (Giambiagi *et al.* 2001). In this instance, however, the narrow width of the fold–thrust belt (<100 km), the low magnitude of shortening (15–45 km) and the strong influence of pre-existing Mesozoic normal faults (e.g. the Malargüe fold–thrust system; Manceda and Figueroa 1995; Giambiagi *et al.* 2008, 2012; Turienzo 2010; Fuentes *et al.* 2016) are insufficient to drive the required >100 km lateral migration of the foreland subsidence profile (flexural wave).

Climate change or sea-level fall (Fig. 3f)

A shift to a humid climate may have promoted heightened erosion and highly efficient sediment transport across the foreland, to such an extreme as to leave no deposits, but only an abandonment surface and gravel lag. This mechanism would involve a major mismatch between the sediment transport capacity and accommodation, and would require large-magnitude exhumation in the thrust belt. To date, the available fission track and U–Th/He thermochronological results show no enhanced exhumation during the 40–20 Ma window (Folguera *et al.* 2015*b*; Bande *et al.* 2020).

Alternatively, an Oligocene drop in base level may partially account for the negligible accumulation in the Argentina foreland (Fuentes and Horton 2020). Although this lowstand would briefly suppress accommodation at a regional scale, this mechanism alone would be insufficient to account for the long duration and virtually complete elimination of accommodation across the foreland from the middle Eocene to earliest Miocene.

Reduced accommodation during tectonic quiescence or oblique deformation (Fig. 3d, e)

The preferred interpretation for the 'Rodados Lustrosos' gravel lag and associated 20 myr hiatus is a prolonged cessation of shortening and flexural loading. The elimination of accommodation would have led to abandonment of the foreland basin, with long-distance sediment transport and/or long residence times for recycled coarse material from the inactive thrust belt. Isolated palaeovalley formation suggests local erosion, potential reflecting a drop in base level or some degree of isostatic rebound. Of particular importance is the absence of a structural or thermochronological record of contemporaneous shortening. Instead, the 40–20 Ma time frame coincided with a period of modest hinterland extension of the Andean orogenic belt at these latitudes (Jordan *et al.* 2001*b*; Burns *et al.* 2006; Charrier *et al.* 2007; Folguera *et al.* 2010; Rojas Vera *et al.* 2014).

In summary, the mid-Cenozoic disconformity in the Neuquén Basin of west-central Argentina (Fig. 5b) is thought to reflect a sustained pause in flexural subsidence that resulted in no net accumulation across an inactive foreland basin, which may be attributable to the cessation of sediment transport or, more likely, to basinwide sediment bypass (Legarreta and Uliana 1991; Horton and Fuentes 2016). In this example, any viable geodynamic mechanisms for foreland quiescence must account for a coeval shift to a neutral or extensional tectonic regime in the corresponding hinterland regions. In the absence of high topography and a thickened crust suitable for gravitational collapse (e.g. Giovanni et al. 2010; Horton 2012), a favoured option is a reduction in mechanical coupling stemming from slab steepening, trench rollback or a decrease in the overriding plate velocity (Maloney et al. 2013; Horton 2018b).

Paleogene erosional unconformity, Magallanes-Austral Basin, southernmost Chile and Argentina

A Paleogene unconformity spanning 15–20 myr is marked by an erosional surface within the Magallanes–Austral foreland basin (Fig. 4). The unconformity (Fig. 5c, d) is situated within the intermediate to upper levels of the 5–7 km thick Upper Cretaceous through Cenozoic foreland succession. The erosional surface incises upper Maastrichtian to lower Paleocene shelf-edge deltaic deposits of the Dorotea and Cerro Dorotea formations and is capped by middle Eocene shallow marine and estuarine deposits of the Man Aike and Rio Turbio formations and the equivalent local units (Fig. 5c, d).

The stratigraphic discontinuity can be traced in surface and subsurface datasets over c. 700 km along strike, from 47 to 54° S. Over

much of its extent, the hiatus spans *c*. 15–20 myr, from the early Paleocene through middle Eocene (Fig. 5c). However, the duration varies significantly from north to south, with regional diachroneity defined by a local maximum hiatus of *c*. 40–60 myr in the north (from Lago Pueyrredón to Lago Viedma at 47–50° S; Fig. 5d) and a continuous Paleocene–Eocene section in the south (within Tierra del Fuego at 53–55° S) (Biddle *et al.* 1986; Ramos 1989; Wilson 1991; Malumián 2002; Ghiglione *et al.* 2014; Sickmann *et al.* 2018; Ronda *et al.* 2019; Fosdick *et al.* 2020; George *et al.* 2020).

Although the Paleogene unconformity lacks an extensive angular discordance, Fosdick *et al.* (2011) interpreted 'a subtle angular unconformity' in selected seismic data. The unconformity cuts across different horizons in the underlying stratigraphic units, suggesting erosional relief exceeding several tens of metres. Although the eroded thickness of the former overburden has been estimated at *c.* 5 km (Fosdick *et al.* 2015), vitrinite reflectance data indicate limited erosion, with the removal of no more than *c.* 500 m during the formation of the unconformity (George *et al.* 2020).

A range of possible geodynamic mechanisms may explain the diachronous Paleogene unconformity in the Magallanes–Austral Basin at 47–54° S. With no clear preference, the choices include: (1) shortening in the proximal foreland; (2) forebulge growth and advance; (3) isostatic rebound during tectonic quiescence; (4) regional uplift during flat-slab subduction; and (5) uplift associated with slab window formation or slab break-off.

Shortening in the proximal foreland (Fig. 3a)

The erosional unconformity may be part of a regional growth structure linked to syndepositional shortening in the frontal zone of the east-directed Patagonian fold—thrust belt (Fosdick *et al.* 2014). Although younger Neogene growth strata are preserved in units above the unconformity (Malumián *et al.* 2000; Ghiglione *et al.* 2016a), the absence of thickness variations or pronounced angular discordance within the Paleogene succession, and the lack of a candidate contractional structure, suggests that localized thrust belt shortening was not responsible for the regional hiatus. The spatial continuity of the preserved erosion surface over hundreds of kilometres would also require a structure of exceptional strike length, which is incompatible with mapped features.

Forebulge growth and advance (Fig. 3b)

A cratonward-advancing forebulge linked to the Patagonian fold—thrust belt could produce an erosional unconformity of long duration and large spatial extent (Wilson 1991). In this explanation, the forebulge unconformity would overlie a thin accumulation of distal backbulge deposits (Figs 1a and 2a), which conflicts with the large (>4 km) thickness of the underlying Upper Cretaceous foreland basin succession. In addition, the required magnitude of lateral migration (>100 km) is inconsistent with the reported values of crustal shortening, which are generally <30–40 km (Alvarez-Marrón *et al.* 1993; Fosdick *et al.* 2011).

Isostatic rebound during tectonic quiescence (Fig. 3d, e)

A termination of shortening and crustal loading would be sufficient to induce erosional unloading of the foreland basin and generate a regional unconformity (George *et al.* 2020). Testing this hypothesis is inhibited by the absence of direct age control on any candidate structures that may have been active during Late Cretaceous to early Eocene time. Reported shifts in Paleogene exhumation and provenance (e.g. Fosdick *et al.* 2020) permit, but do not require, synchronous deformation. Direct structural timing constraints are necessary to better separate phases of non-deposition from the regional effects of sea-level lowstands (Malumián 2002; Olivero and Malumián 2008).

Regional uplift during flat-slab subduction (Fig. 3g)

A potential decline or termination of arc magmatism at roughly 65–45 Ma may reflect a phase of Paleogene flat-slab subduction, as proposed farther north for northern Patagonia at 40–46° S (Gianni et al. 2018; Horton 2018b; Butler et al. 2020). George et al. (2020) point to an apparent lull in arc magmatism at 60–45 Ma on the basis of detrital zircon age distributions at 50–51° S, which would be consistent with an extinguished arc during shallow subduction. If sufficient geochronological and geochemical datasets for Patagonia were available, then the history of subduction-related arc magmatism could be discriminated from intraplate magmatism to identify any inboard progression of arc magmatism.

Uplift associated with slab window formation or slab break-off (Fig. 3h)

Paleogene slab window development has been discussed for a northern region (44–51° S), where diminished arc magmatism coincided with a phase of intraplate magmatism fed by primitive mantle sources (as represented by extrusive units such as the middle Eocene Posadas basalt; Fig. 5d). In this region, collision of the Aluk-Farallon spreading ridge led to progressive Eocene (roughly 57–40 Ma) opening of a slab window (Ramos 2005; Aragón *et al.* 2013; Gianni *et al.* 2018). Although the Eocene time frame partially overlaps with the hiatus in the Magallanes–Austral Basin at 47–54° S, the predicted timing of slab window formation at more southern latitudes would be substantially younger, by up to 10 myr. Therefore, although the hypothesis would be consistent with the possible 60–45 Ma lull in arc magmatism (George *et al.* 2020), this diachroneity of slab window opening and incomplete records of intraplate magmatism present challenges to this interpretation.

Late Cenozoic sediment bypass in the Patagonian foreland, southern Argentina

The Patagonian fold-thrust belt at 43–53° S (Fig. 4) is flanked to the east by a low-relief erosional plain that is no longer an actively subsiding foreland basin (Fig. 5d). This retroarc landscape of Argentina includes flat-lying Cretaceous-Cenozoic foreland basin

strata that are now undergoing widespread erosion (Ramos 1989, 2005; Bouza and Bilmes 2020). The relict foreland contains an anomalously high topography (roughly 500 m above sea-level), the highest Andean retroarc region (Fig. 4) that is not directly linked to upper crustal faulting. Modest regional uplift across this narrow continental strip is registered by late Miocene–Quaternary fluvial and marine terraces up to several hundred metres above sea-level (Feruglio 1950; Guillaume *et al.* 2009; Pedoja *et al.* 2011).

The switch from foreland subsidence to regional erosion occurred in the middle Miocene at c. 15 Ma (Fig. 5c, d; Ghiglione et al. 2016b; Dávila et al. 2019; Fosdick et al. 2020). Although the retroarc region ceased to accommodate and preserve sedimentary deposits, this did not prohibit the production and transport of clastic sediments across the abandoned foreland basin. Large-scale exhumation of the fold-thrust belt through fluvial and aeolian processes since c. 15 Ma and active glaciation since c. 6 Ma have supplied considerable sediment to the eastern plains (Thomson et al. 2001; Guillaume et al. 2013; Ghiglione et al. 2019; Willett et al. 2020). This sediment has bypassed the relict foreland to be deposited farther east in the offshore Argentine and Malvinas basins of the Atlantic passive margin (Fig. 4; Ghiglione et al. 2016b). The onshore record of sediment bypass is represented by an abandonment surface capped by a thin (<10-20 m thick), but extensive, gravel lag, the 'Rodados Patagónicos' (Feruglio 1950; Parras et al. 2008; Ghiglione et al. 2016b; Barberón et al. 2019; Bouza and Bilmes 2020), which Darwin (1842) referred to as the 'Patagonian Shingle Formation' (Martínez et al. 2009).

Folguera *et al.* (2015*a*) outlined possible geodynamic controls on the modern foreland configuration; most are encapsulated in the unconformity generation mechanisms summarized previously (Fig. 3). In the Patagonian foreland at 43–53° S, basin abandonment corresponds with the opening of an active slab window (Fig. 3h). Both the Patagonian Andes and adjacent foreland show an abrupt topographic step that overlaps with the position of the Chile triple junction at 46° S (Fig. 7). Ramos (2005) attributed the elevated topography to enhanced dynamic uplift linked to northward progression of the Nazca–Antarctic spreading ridge (the Chile Ridge) to where it now intersects the trench at 46° S (Figs 4 and 7). In this context, a slab window has opened over the past *c.* 16 myr

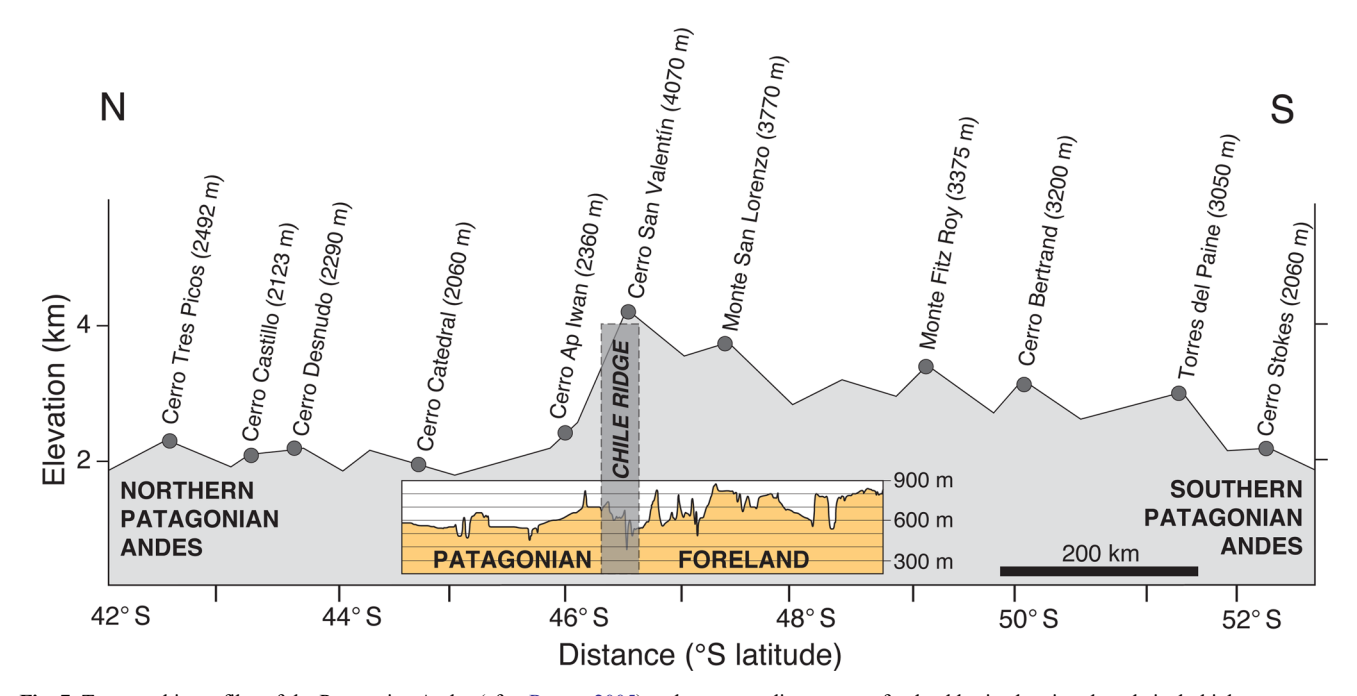


Fig. 7. Topographic profiles of the Patagonian Andes (after Ramos 2005) and corresponding retroarc foreland basin showing the relatively higher mean topography and topographic relief south of the Chile Ridge (the Nazca–Antarctic spreading ridge), which has advanced northward through time. Map-view profile traces are shown in Figure 4; stratigraphic framework is shown in Figure 5c, d.

Unconformities and geodynamics of foreland basins

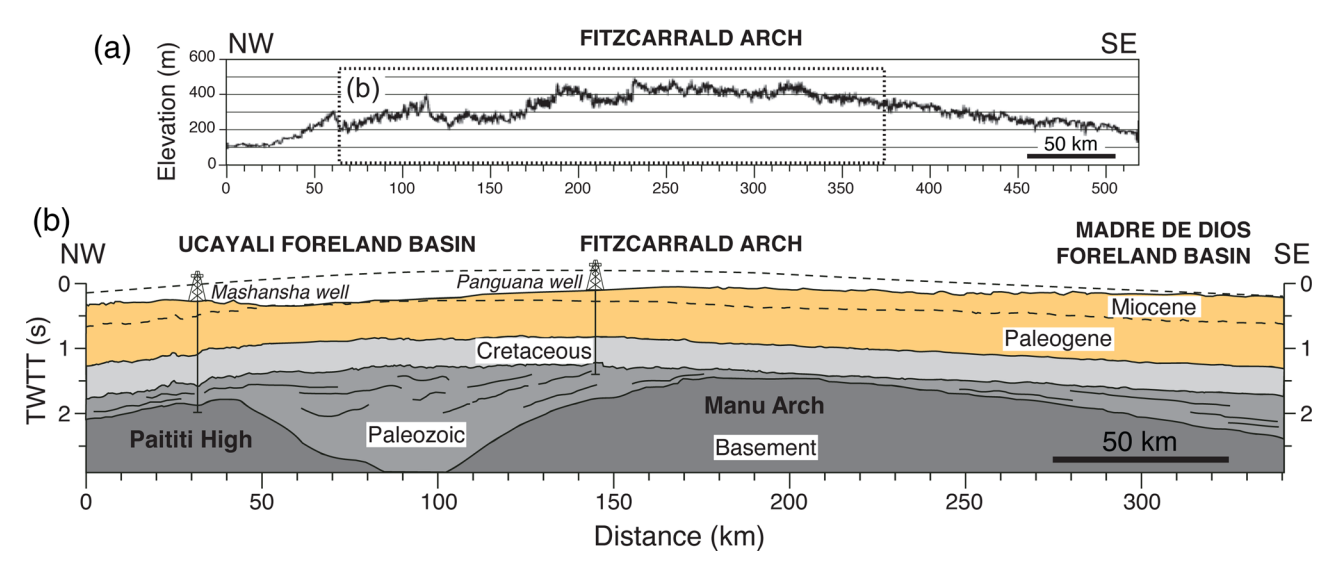


Fig. 8. Profiles of the Fitzcarrald Arch (Figs 4 and 5e) along the boundary between the Ucayali Basin and Madre de Dios Basin, Peru (after Espurt *et al.* 2007, 2010). (a) Regional topographic profile showing the *c.* 500 km wavelength of the uplifted Fitzcarrald Arch. (b) Seismic reflection profile showing the broad warping of the basement and the overlying Phanerozoic strata, as well as the erosional removal of the Neogene strata.

and now underlies the Patagonian foreland from 46 to 55° S (Lagabrielle *et al.* 2004; Breitsprecher and Thorkelson 2008). This geodynamic history contrasts with the rest of the Andes. Therefore, rather than focused crustal thickening (e.g. Stevens Goddard and Fosdick 2019), regional uplift and accommodation reduction along this segment of the Andean margin can be attributed to dynamic mantle processes (Fig. 3h) (Guillaume *et al.* 2009; Folguera *et al.* 2015*a*; Dávila *et al.* 2019).

Late Cenozoic flat-slab subduction beneath the Ucayali Basin, central Peru

The flat-slab province of Peru provides an opportunity to judge the retroarc response to a rapid shift from steep to shallow subduction, a potential mechanism for regional unconformity development in foreland basins (Fig. 3g). The modern zone of flat-slab subduction at 4–15° S is linked to subduction of the buoyant Nazca Ridge (Fig. 4), an aseismic ridge that intersected the margin at *c*. 10 Ma in northern Peru and swept progressively southward to its current location in southern Peru (Hampel 2002; Rosenbaum *et al.* 2005; Ramos and Folguera 2009; Antonijevic *et al.* 2015).

The modern foreland basin of Peru consists of actively subsiding, low-elevation (<100–150 m) plains flanked by the Andean fold—thrust belt (Dumont 1996; Mora et al. 2010). The different geographical designations within the Peruvian (Amazonian) foreland – including the Marañon, Ucayali and Madre de Dios basins – contain comparable stratigraphic records showing large-volume sediment accumulation during the Miocene–Pliocene (Fig. 5e) (Espurt et al. 2010, 2011; Roddaz et al. 2010; Antoine

et al. 2016; Iribarne et al. 2018; Zamora and Gil 2018). A critical departure from this trend exists in the Ucavali Basin at roughly 8-12° S, where large-wavelength uplift of Miocene-Pliocene foreland basin fill is expressed in topographic, stratigraphic and structural data (Espurt et al. 2007, 2010). This anomalous region constitutes the Fitzcarrald Arch, a 400 000 km² foreland zone situated at c. 600 m above sea-level, considerably higher than the subsiding plains of the flanking northern (Ucayali) and southern (Madre de Dios) sectors of the modern basin (Fig. 4). Although this elevated region in the proximal foreland could be argued to represent an aggradational fluvial megafan similar to other Andean settings (e.g. Räsänen et al. 1992; Horton and DeCelles 2001), surface and subsurface geometries showing broad-wavelength (300-600 km) warping of Miocene-Pliocene stratigraphic units since c. 4 Ma (Fig. 8) demonstrate a structural origin for the Fitzcarrald Arch (Espurt et al. 2007, 2010; Regard et al. 2009). Moreover, the present drainage catchment geometries reveal an increase in relief from fluvial incision (Regard et al. 2009) rather than the topographic levelling that would be expected for megafan construction during aggradation in a subsiding foreland basin.

The temporal and spatial correspondence of the subducted Nazca Ridge and the Fitzcarrald Arch (Fig. 4) indicate the vital role of flat-slab subduction in driving a reversal from foreland aggradation to degradation. Although uncertainty remains in gauging the exact processes responsible, the increased buoyancy of the aseismic ridge likely caused slab shallowing, which, in turn, led to increased mechanical coupling along the contact between the subducting and overriding plates (Gutscher *et al.* 2000; Martinod *et al.* 2010; Bishop *et al.* 2018). The foreland response to Nazca Ridge

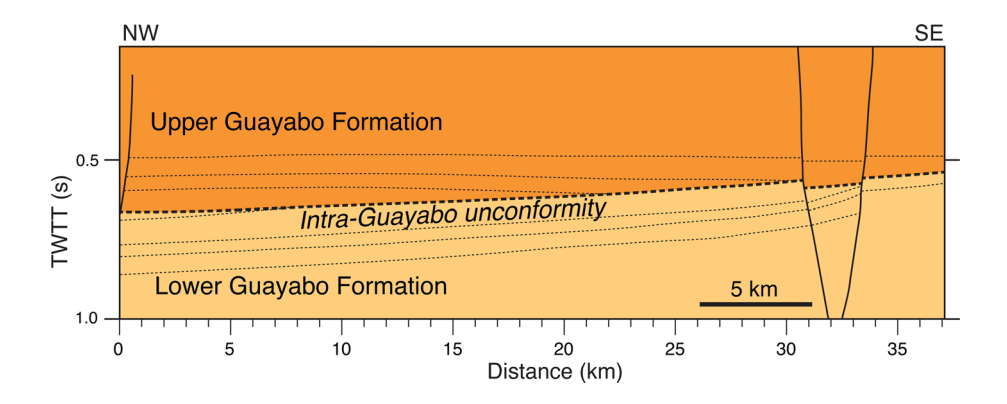


Fig. 9. Line tracing of a seismic reflection profile in the Llanos Basin, Colombia showing an unconformity within the upper Miocene–Pliocene Guayabo Formation (after Delgado *et al.* 2012). The intra-Guayabo unconformity indicates erosional truncation of the underlying NW-dipping reflectors (dipping toward the orogen) and progressive onlap by overlying reflectors toward the SE (toward the craton), consistent with rapid regional tilting.

subduction has been regional dynamic uplift (i.e. wholesale uplift in the absence of crustal thickening) that exceeds the coeval flexural subsidence due to shortening in the Andean fold–thrust belt (Fig. 3g).

Late Cenozoic regional tilting in the Llanos Basin, Colombia

The Pliocene-Quaternary record of the Llanos foreland basin in Colombia (Fig. 4) is linked to the geodynamic evolution of the northern Andes. Using an extensive subsurface dataset, Delgado et al. (2012) defined an intrabasinal unconformity that suggests a major shift in foreland accommodation. The unconformity occurs in proximal to medial segments of the Llanos Basin within intermediate levels of the c. 3-4 km thick upper middle Miocene-Pliocene Guayabo Formation (Fig. 5f). This intra-Guayabo unconformity exhibits low-angle discordance over tens of kilometres. Seismic images reveal initial erosional bevelling of older strata that dip gently toward the orogen (northwestward) followed by progressive cratonal (southeastward) onlap of the unconformity surface by younger strata (Fig. 9). This geometry is consistent with sharply asymmetrical subsidence, with rapid regional tilting toward the Andean thrust front accompanied by erosion in more distal parts of the basin, potentially including a broad forebulge or cratonic margin. Multiple small-offset normal faults may have helped facilitate regional tilting (Delgado et al. 2012).

Limited age control prevents a clear understanding of the duration of the intraformational hiatus. Regional correlations and past estimates suggest a late Miocene to mid-Pliocene age for the Guayabo Formation (Cooper *et al.* 1995; Mora *et al.* 2008; Parra *et al.* 2009, 2010; Bande *et al.* 2012; Reyes-Harker *et al.* 2015). The precise age of the discordance, although speculative, is inferred to be within the 7.1–4.8 Ma range (Fig. 5f), the reported age of the T-17 palynological biozone (Duarte *et al.* 2017; Jaramillo *et al.* 2017). The actual hiatus may be markedly shorter than this 2.3 myr time frame.

Several possible interpretations warrant consideration. A latest Miocene–early Pliocene age for the intra-Guayabo discordance matches the proposed timing of initial flat-slab subduction beneath the Colombian Andes (Wagner *et al.* 2017). Establishment of this flat-slab configuration at 2–7° N (Fig. 4) may have prompted a pulse of basement-involved shortening within the foreland. However, unlike other proposals of wholesale regional uplift during subduction shallowing, the unconformity geometry would require spatially variable uplift that imparted a regional tilt to the basin prior to erosional bevelling (Fig. 9).

Separately, the apparent time frame for unconformity generation overlapped with reported increases in thrust belt shortening, mean elevation, orographic rainfall and erosional exhumation (Mora *et al.* 2008, 2013). These factors may have led to heightened topographic loading, greater subsidence and, with an increased sediment supply, prospective overfilling of the Llanos foreland basin. Depending on the distribution of tectonic and sedimentary loads, these processes may also have induced a modest retreat of the forebulge or distal basin margin toward the thrust belt, accentuating regional tilting and further promoting unconformity growth in the proximal to medial foreland.

Discussion

The examples presented here provide insights into the geodynamic mechanisms of unconformity development in foreland basins. Consideration of modern and ancient examples helps promote a workflow that evaluates multiple possible explanations (Fig. 3), recognizing the potential for separate mechanisms to operate simultaneously. This paper emphasizes lengthy stratigraphic

discontinuities, which require a severe reduction or elimination of accommodation over geological time frames. This involves (1) erosion, (2) sediment bypass with the transport of materials to more distal regions or (3) the extremely slow accumulation of a condensed stratigraphic interval (Figs 1 and 2). A single locality may fluctuate among these three modes.

This discussion emphasizes criteria pertaining to the interpretation of unconformity generation mechanisms in Andean-type retroarc settings. These mechanisms can be distinguished on the basis of the spatial extent, structural situation, stratigraphic position, palaeoenvironmental conditions and duration of the unconformities and condensed sections within the broader tectonic context of the convergent margin.

Spatial extent and relationship with identified structures

The geographical distribution, along-strike continuity and geometric relationships with surface or subsurface structures are essential observables. Is the spatial extent of the unconformity compatible with known features, such as a frontal fold—thrust structure (Fig. 3a), a broad flexural forebulge (Fig. 3b) or an intraforeland basement block uplift (Fig. 3c)? The magnitude of any angular discordance, along with correlations of age-equivalent strata and assessments of lateral thickness variations, will aid in the recognition of synorogenic growth strata linked to individual structures. Using this rationale, we can readily dismiss proposed structural controls in circumstances where discernible structures are absent or identified structures are of insufficient strike length, displacement magnitude or time span to account for the location and extent of the unconformity in question.

Age, duration and potential diachroneity of an unconformity

Information on the age and duration of a stratigraphic discontinuity will help to distinguish short-term eustatic, climatic or autogenic fluctuations (Fig. 3f) from longer term forcings. Several mechanisms are time-transgressive, such as the cratonward migration of a flexural forebulge during propagation of an orogenic wedge (Fig. 3b), or the progressive inboard advance of a flat slab during subduction shallowing (Fig. 3g). The unconformity or condensed section created by such diachronous processes must be compatible with the reconstructed topographic loads, mechanical properties of the foreland lithosphere, and records of deformation and magmatism. Further, the duration of the hiatus may be highly variable, as in episodes of isostatic rebound where greater erosional removal in the proximal foreland yields a stratigraphic gap of diminishing age toward the distal foreland (Fig. 3d, e).

Stratigraphic and palaeoenvironmental history before and after unconformity development

Determining whether an unconformity or condensed interval is positioned at the base or internally within the foreland basin succession is necessary for proper interpretation (Fig. 2). This distinction resolves whether a stratigraphic discontinuity may mark the inception of orogenesis or some later synorogenic process. In assessing unconformity genesis, the preserved rock records directly above and below the unconformity (or the facies within a condensed section) provide an unambiguous record of accommodation variations immediately before, after and potentially during the hiatus. The relative magnitude of accommodation interruption will scale differently for the potential drivers. Changes in sea-level, climate or erosion (Fig. 3f) will also produce recognizable shifts in palaeoenvironments and sediment transport parameters reflected in the preserved facies.

Tectonic regimes within the flanking orogenic belt

Plate reconstructions and deformational histories inform geological analyses of foreland basin evolution. One challenge for contractional systems involves periods in which shortening may cease or be greatly lessened. During a shutdown in shortening, the tectonic regime of the orogen may shift to neutral conditions, a tensile mode with hinterland extension (Fig. 3d) or margin-wide strike-slip deformation (Fig. 3e), any of which would induce basin abandonment. The time–space relationships between unconformity development and magmatism are further valued because a pause in subduction-related arc magmatism can reflect (1) a tectonic shift to an oblique, translational or transpressional orogenic system (Fig. 3e), (2) flat-slab subduction (Fig. 3g) or (3) slab window formation (Fig. 3h).

Time-stratigraphic relationships

In evaluating different options, chronostratigraphic cross-sections (Wheeler diagrams) prove effective in documenting lateral and vertical relationships within the stratigraphic record (Fig. 2). These constraints stimulate estimates of the potential relationships to crustal structures or broader geodynamic elements of the orogenic system. Even where the underlying mechanisms of unconformity generation are not apparent, such time—space assessments are useful in discriminating among viable explanations. In practice, this regularly helps catalyse a discussion of alternative interpretations. For example, the identification of contrasting stratigraphic intervals of comparable age permits the isolation of key variables to better understand why an unconformity or condensed section formed in one region, but not in another.

Modern analogues

Interpretations of foreland basin unconformities and condensed sections can be challenging, as demonstrated by ancient examples from the Andes (Figs 4 and 5). For the cases described, there are multiple possibilities (Fig. 3) and debate commonly focuses on specific field relationships, stratigraphic correlations or age control within the basin (Fig. 5). Some explanations are mutually exclusive, but others are not.

Case studies from the modern Andean foreland provide greater clarity regarding what may otherwise involve complex or non-unique explanations. These observations address the current plate configuration (Fig. 4) and active foreland basin processes in terms of erosion, sediment bypass or subsidence, enabling interpretations with higher confidence. For the late Cenozoic situations considered, the effects of subduction-related parameters are clear, such that the foreland responses can be observed directly in instances of flat-slab subduction, ocean ridge subduction and slab window generation (Figs 3g, h, 7 and 8). Enhanced exploration of the late Cenozoic to present day foreland conditions will help to improve the ability to accurately reconstruct the geodynamic evolution of ancient convergent margins from the foreland basin stratigraphic record.

Acknowledgements Reviewers German Bayona and Matías Ghiglione provided constructive comments that improved this paper. Discussions with Ryan Anderson, Amanda Calle, Tomas Capaldi, Julia Clarke, Kurt Constenius, Andrés Folguera, Facundo Fuentes, Sarah George, Lily Jackson, Chelsea Mackaman-Lofland, Andrés Mora, Mauricio Parra, Nicholas Perez, Sebastian Ramirez, Zachary Sickmann and Daniel Starck helped clarify the presentation.

Author contributions BKH: conceptualization (lead), funding acquisition (lead), investigation (lead), writing – original draft (lead), writing – review & editing (lead)

Funding This work was funded by the National Science Foundation (EAR-1918541, EAR-1925898 and EAR-1946700).

Data availability Data sharing is not applicable to this article as no dataset was generated or analysed during the current study.

Scientific editing by Feng Cheng

References

- Aleman, A. and Ramos, V.A. 2000. The northern Andes. In: Cordani, U.G., Milani, E.J., Thomaz Filho, A. and Campos Neto, M.C. (eds) Tectonic Evolution of South America. Institut de Recherche pour le Développement, International Geological Congress, Rio de Janeiro, 31, 453–480.
- Allen, P.A., Armitage, J.J. et al. 2013. The Qs problem: sediment volumetric balance of proximal foreland basin systems. Sedimentology, 60, 102–130, https://doi.org/10.1111/sed.12015
- Allmendinger, R.W. and Judge, P.A. 2014. The Argentine Precordillera: a foreland thrust belt proximal to the subducted plate. *Geosphere*, **10**, 1203–1218, https://doi.org/10.1130/GES01062.1
- Allmendinger, R.W., Loveless, J.P., Pritchard, M.E. and Meade, B. 2009. From decades to epochs: spanning the gap between geodesy and structural geology of active mountain belts. *Journal of Structural Geology*, 31, 1409–1422, https://doi.org/10.1016/j.jsg.2009.08.008
- Alvarez-Marrón, J., McClay, K., Harambour, S., Rojas, L. and Skarmeta, J. 1993. Geometry and evolution of the frontal part of the Magallanes foreland thrust and fold belt (Vicuña area), Tierra del Fuego, southern Chile. AAPG Bulletin, 77, 1904–1921.
- Anadón, P., Cabrera, L., Colombo, F., Marzo, M. and Riba, O. 1986. Syntectonic intraformational unconformities in alluvial fan deposits, eastern Ebro Basin margins (NE Spain). *International Association of Sedimentologists, Special Publications*, 8, 259–271.
- Anderson, R.B., Long, S.P., Horton, B.K., Thomson, S.N., Calle, A.Z. and Stockli, D.F. 2018. Orogenic wedge evolution of the central Andes, Bolivia (21°S): implications for Cordilleran cyclicity. *Tectonics*, 37, 3577–3609, https://doi.org/10.1002/2018TC005132
- Andeweg, B. and Cloetingh, S. 1998. Flexure and 'unflexure' of the North Alpine German–Austrian Molasse basin: constraints from forward tectonic modelling. *Geological Society, London, Special Publications*, 134, 403–422, https://doi.org/10.1144/GSL.SP.1998.134.01.19
- Antoine, P.O., Abello, M.A. *et al.* 2016. A 60-million-year Cenozoic history of western Amazonian ecosystems in Contamana, eastern Peru. *Gondwana Research*, **31**, 30–59, https://doi.org/10.1016/j.gr.2015.11.001
- Antonijevic, S.K., Wagner, L.S. et al. 2015. The role of ridges in the formation and longevity of flat slabs. *Nature*, **524**, 212–215, https://doi.org/10.1038/ nature14648
- Aragón, E., Pinotti, L. *et al.* 2013. The Farallon–Aluk ridge collision with South America: implications for the geochemical changes of slab window magmas from fore- to back-arc. *Geoscience Frontiers*, **4**, 377–388, https://doi.org/10. 1016/j.gsf.2012.12.004
- Assumpção, M., Dias, F.L., Zevalos, I. and Naliboff, J.B. 2016. Intraplate stress field in South America from earthquake focal mechanisms. *Journal of South American Earth Sciences*, 71, 278–295, https://doi.org/10.1016/j.jsames. 2016.07.005
- Avouac, J.P. 2003. Mountain building, erosion, and the seismic cycle in the Nepal Himalaya. *Advances in Geophysics*, **46**, 1–80, https://doi.org/10.1016/S0065-2687(03)46001-9
- Axen, G.J., van Wijk, J.W. and Currie, C.A. 2018. Basal continental mantle lithosphere displaced by flat-slab subduction. *Nature Geoscience*, **11**, 961–964, https://doi.org/10.1038/s41561-018-0263-9
- Balkwill, H.R., Rodrigue, G., Paredes, F.I. and Almeida, J.P. 1995. Northern part of Oriente basin, Ecuador: reflection seismic expression of structures. AAPG Memoirs, 62, 559–571.
- Bally, A.W., Gordy, P.L. and Stewart, G.A. 1966. Structure, seismic data and orogenic evolution of the southern Canadian Rockies. *Bulletin of Canadian Petroleum Geology*, 14, 337–381.
- Bande, A., Horton, B.K., Ramírez, J.C., Mora, A., Parra, M. and Stockli, D.F. 2012. Clastic deposition, provenance, and sequence of Andean thrusting in the frontal Eastern Cordillera and Llanos foreland basin of Colombia. GSA Bulletin, 124, 59–76, https://doi.org/10.1130/B30412.1
- Bande, A., Boll, A., Fuentes, F., Horton, B.K. and Stockli, D.F. 2020. Thermochronological constraints on the exhumation of the Malargüe fold–thrust belt, southern Central Andes. *In:* Kietzmann, D. and Folguera, A. (eds) *Opening and Closure of the Neuquén Basin in the Southern Andes.* Springer Earth System Sciences, 371–396, https://doi.org/10.1007/978-3-030-29680-3 14
- Barberón, V., Sue, C., Ghiglione, M., Ronda, G. and Aragón, E. 2018. Late Cenozoic brittle deformation in the Southern Patagonian Andes: record of plate coupling/decoupling during variable subduction? *Terra Nova*, 30, 296–309, https://doi.org/10.1111/ter.12339
- Barberón, V., Ronda, G. et al. 2019. Tectonic evolution of the northern Austral–Magallanes basin in the southern Patagonian Andes from provenance analysis. Journal of South American Earth Sciences, 95, 102234, https://doi.org/10.1016/j.isames.2019.102234
- Barnes, J.B., Ehlers, T.A., McQuarrie, N., O'Sullivan, P.B. and Pelletier, J.D. 2006. Eocene to Recent variations in erosion across the central Andean fold—

thrust belt, northern Bolivia: implications for plateau evolution. *Earth and Planetary Science Letters*, **248**, 118–133, https://doi.org/10.1016/j.epsl.2006.

- Barrell, J. 1917. Rhythms and the measurements of geologic time. *GSA Bulletin*, **28**, 745–904, https://doi.org/10.1130/GSAB-28-745
- Bayona, G. and Thomas, W.A. 2003. Distinguishing fault reactivation from flexural deformation in the distal stratigraphy of the peripheral Blountian foreland basin, southern Appalachians, USA. *Basin Research*, **15**, 503–526, https://doi.org/10.1046/j.1365-2117.2003.00217.x
- Bayona, G. and Thomas, W.A. 2006. Influence of pre-existing plate-margin structures and stratigraphy on foredeep filling: insights from the Taconian (Blountian) clastic wedge, southeastern USA. Sedimentary Geology, 119, 115–133, https://doi.org/10.1016/j.sedgeo.2006.02.001
- Bayona, G., Cortes, M., Jaramillo, C., Ojeda, G., Aristizabal, J. and Reyes-Harker, A. 2008. An integrated analysis of an orogen-sedimentary basin pair: latest Cretaceous-Cenozoic evolution of the linked Eastern Cordillera orogen and the Llanos foreland basin of Colombia. GSA Bulletin, 120, 1171–1197, https://doi.org/10.1130/B26187.1
- Bayona, G., Baquero, M. et al. 2020. Unravelling the widening of the earliest Andean northern orogen: Maastrichtian to early Eocene intra-basinal deformation in the northern Eastern Cordillera of Colombia. Basin Research, 33, 809–845, https://doi.org/10.1111/bre.12496
- Beaumont, C. 1981. Foreland basins. *Geophysical Journal of the Royal Astronomical Society*, **65**, 291–329, https://doi.org/10.1111/j.1365-246X. 1981.tb02715.x
- Beaumont, C., Muñoz, J.A., Hamilton, J. and Fullsack, P. 2000. Factors controlling the Alpine evolution of the central Pyrenees inferred from a comparison of observations and geodynamical models. *Journal of Geophysical Research*, 105, 8121–8145, https://doi.org/10.1029/1999JB900390
- Biddle, K.T., Uliana, M.A., Mitchum, R.M.,Jr, Fitzgerald, M.G. and Wright, R.C. 1986. The stratigraphic and structural evolution of the central and eastern Magallanes Basin, southern South America. *International Association of Sedimentologists, Special Publications*, 8, 41–61.
- Bird, P. 1984. Formation of the Rocky Mountains foreland and Great Plains. *Tectonics*, **3**, 741–758, https://doi.org/10.1029/TC003i007p00741
- Birot, P. 1937. Recherches sur la morphologie des Pyrénées orientales Francoespagnoles. PhD thesis, Université de Paris, Baillière et Fils.
- Bishop, B.T., Beck, S.L., Zandt, G., Wagner, L.S., Long, M.D. and Tavera, H. 2018. Foreland uplift during flat subduction: insights from the Peruvian Andes and Fitzcarrald Arch. *Tectonophysics*, 731–732, 73–84, https://doi.org/10. 1016/j.tecto.2018.03.005
- Blackwelder, E. 1909. The valuation of unconformities. *Journal of Geology*, **17**, 289–299, https://doi.org/10.1086/621610
- Blisniuk, P.M., Stern, L.A., Chamberlain, C.P., Idleman, B. and Zeitler, P.K. 2005. Climatic and ecologic changes during Miocene surface uplift in the southern Patagonian Andes. *Earth and Planetary Science Letters*, 230, 169–186, https://doi.org/10.1016/j.epsl.2004.11.015
- Boll, A. and Hernández, R.M. 1986. Interpretación estructural del área Tres Cruces. Boletín de Informaciones Petroleras, 7, 2–14.
- Boll, A., Alonso, A., Fuentes, F., Vergara, M., Laffitte, G. and Villar, H.J. 2014. Factores controlantes de las acumulaciones de hidrocarburos en el sector norte de la cuenca Neuquina, entre los ríos Diamante y Salado, Provincia de Mendoza, Argentina. *In*: Cruz, C.E., Fantin, F. et al. (eds) IX Congreso de Exploración y Desarrollo de Hidrocarburos, Mendoza, Argentina, 3–44.
- Bourgois, J., Guivel, C., Lagabrielle, Y., Calmus, T., Boulegue, J. and Daux, V. 2000. Glacial-interglacial trench supply variation, spreading-ridge subduction, and feedback controls on the Andean margin development at the Chile triple junction area (45–48°S). *Journal of Geophysical Research*, 105, 8355–8386, https://doi.org/10.1029/1999JB900400
- Bouza, P.J. and Bilmes, A. 2020. Landscapes and geology of Patagonia: an introduction to the land of reptiles. *In*: Morando, M. and Avila, L.J. (eds) *Lizards of Patagonia: Diversity, Systematics, Biogeography and Biology of the Reptiles at the End of the World.* Springer, 59–83, https://doi.org/10.1007/978-3-030-42752-8_4
- Breitsprecher, K. and Thorkelson, D.J. 2008. Neogene kinematic history of Nazca–Antarctic–Phoenix slab windows beneath Patagonia and the Antarctic Peninsula. *Tectonophysics*, **464**, 10–20, https://doi.org/10.1016/j.tecto.2008.02.013
- Burns, W.M., Jordan, T.E., Copeland, P. and Kelley, S.A. 2006. The case for extensional tectonics in the Oligocene–Miocene southern Andes as recorded in the Cura Mallín basin (36°–38°S). *GSA, Special Papers*, **407**, 163–184, https://doi.org/10.1130/2006.2407(08)
- Burov, E. and Cloetingh, S. 2009. Controls of mantle plumes and lithospheric folding on modes of intraplate continental tectonics: differences and similarities. *Geophysical Journal International*, 178, 1691–1722, https://doi. org/10.1111/j.1365-246X.2009.04238.x
- Butler, K.L., Horton, B.K., Echaurren, A., Folguera, A. and Fuentes, F. 2020. Cretaceous–Cenozoic growth of the Patagonian broken foreland basin, Argentina: chronostratigraphic framework and provenance variations during transitions in Andean subduction dynamics. *Journal of South American Earth Sciences*, 97, 102242, https://doi.org/10.1016/j.jsames.2019.102242
- Caballero, V.M., Rodríguez, G., Naranjo, J.F., Mora, A. and De La Parra, F. 2020. From facies analysis, stratigraphic surfaces, and depositional sequences to stratigraphic traps in the Eocene–Oligocene record of the southern Llanos Basin and northern Magdalena Basin. *In*: Gómez, J. and Mateus-Zabala, D.

- (eds) *The Geology of Colombia*. Vol. 37. Servicio Geológico Colombiano, Publicaciones Geológicas Especiales, Bogotá, 283–330, https://doi.org/10.32685/pub.esp.37.2019.10
- Calle, A.Z., Horton, B.K., Limachi, R., Stockli, D.F., Uzeda-Orellana, G.V., Anderson, R.B. and Long, S.P. 2018. Cenozoic provenance and depositional record of the Sub-Andean foreland basin during growth of the central Andean fold-thrust belt, southern Bolivia. AAPG Memoirs, 117, 483–530, https://doi. org/10.1306/13622132m1173777
- Cant, D.J. and Stockmal, G.S. 1989. The Alberta foreland basin: relationship between stratigraphy and Cordilleran terrane-accretion events. *Canadian Journal of Earth Sciences*, 26, 1964–1975, https://doi.org/10.1139/e89-166
- Carlotto, V. 2013. Paleogeographic and tectonic controls on the evolution of Cenozoic basins in the Altiplano and Western Cordillera of southern Peru. Tectonophysics, 589, 195–219, https://doi.org/10.1016/j.tecto.2013.01.002
- Carrapa, B. and DeCelles, P.G. 2008. Eocene exhumation and basin development in the Puna of northwestern Argentina. *Tectonics*, 27, TC1015, https://doi.org/ 10.1029/2007TC002127
- Carrapa, B., DeCelles, P.G. and Romero, M. 2019. Early inception of the Laramide orogeny in southwestern Montana and northern Wyoming: implications for models of flat-slab subduction. *Journal of Geophysical Research*, 124, 2102–2123, https://doi.org/10.1029/2018JB016888
- Catuneanu, O., Beaumont, C. and Waschbusch, P. 1997. Interplay of static loads and subduction dynamics in foreland basins: reciprocal stratigraphies and the "missing" peripheral bulge. *Geology*, 25, 1087–1090, https://doi.org/10.1130/ 0091-7613(1997)025<1087:IOSLAS>2.3.CO;2
- Chapman, J.B. and DeCelles, P.G. 2015. Foreland basin stratigraphic control on thrust belt evolution. *Geology*, 43, 579–582, https://doi.org/10.1130/G36597.1
- Charrier, R., Pinto, L. and Rodríguez, M.P. 2007. Tectonostatigraphic evolution of the Andean Orogen in Chile. *In*: Moreno, T. and Gibbons, W. (eds) *The Geology of Chile*. Geological Society, London, 21–114.
- Chase, C.G., Sussman, A.J. and Coblentz, D.D. 2009. Curved Andes: geoid, forebulge, and flexure. *Lithosphere*, 1, 358–363, https://doi.org/10.1130/L67.1
- Christophoul, F., Soula, J., Brusset, S.C., Elibana, B., Roddaz, M., Bessière, G. and Déramond, J. 2003. Time, place and mode of propagation of foreland basin systems as recorded by the sedimentary fill: examples of the Late Cretaceous and Eocene retro-foreland basins of the north-eastern Pyrenees. Geological Society, London, Special Publications, 208, 229–252, https://doi.org/10.1144/GSL.SP.2003.208.01.11
- Clari, P.A., Dela Pierre, F. and Martire, L. 1995. Discontinuities in carbonate successions: identification, interpretation and classification of some Italian examples. *Sedimentary Geology*, **100**, 97–121, https://doi.org/10.1016/0037-0738(95)00113-1
- Clevis, Q., De Boer, P.L. and Nijman, W. 2004. Differentiating the effect of episodic tectonism and eustatic sea-level fluctuations in foreland basins filled by alluvial fans and axial deltaic systems: insights from a three-dimensional stratigraphic forward model. *Sedimentology*, **51**, 809–835, https://doi.org/10.1111/j.1365-3091.2004.00652.x
- Clift, P.D. 2010. Enhanced global continental erosion and exhumation driven by Oligo-Miocene climate change. *Geophysical Research Letters*, 37, L09402, https://doi.org/10.1029/2010GL043067
- Clift, P.D. and Van Laningham, S. 2010. A climatic trigger for a major Miocene unconformity in the Himalayan foreland basin. *Tectonics*, 29, TC5014, https://doi. org/10.1029/2010TC002711
- Cloetingh, S. and Burov, E. 2011. Lithospheric folding and sedimentary basin evolution: a review and analysis of formation mechanisms. *Basin Research*, 23, 257–290, https://doi.org/10.1111/j.1365-2117.2010.00490.x
- Coney, P.J. 1973. Plate tectonics of marginal foreland thrust–fold belts. *Geology*, **1**, 131–134, https://doi.org/10.1130/0091-7613(1973)1 < 131:PTOMFT>2.0.
- Coney, P.J. and Evenchick, C.A. 1994. Consolidation of the American Cordilleras. *Journal of South American Earth Sciences*, 7, 241–262, https://doi.org/10.1016/0895-9811(94)90011-6
- Cooper, M.A., Addison, F.T. et al. 1995. Basin development and tectonic history of the Llanos Basin, Eastern Cordillera, and Middle Magdalena Valley, Colombia. AAPG Bulletin, 79, 1421–1443.
- Costa, C., Alvarado, A. et al. 2020. Hazardous faults of South America; compilation and overview. Journal of South American Earth Sciences, 104, 102837, https://doi.org/10.1016/j.jsames.2020.102837
- Crampton, S.L. and Allen, P.A. 1995. Recognition of flexural forebulge unconformities in the geologic record. *AAPG Bulletin*, **79**, 1495–1514.
- Dahlen, F.A. and Suppe, J. 1988. Mechanics, growth, and erosion of mountain belts. GSA, Special Papers, 218, 161–178.
- Darwin, C.R. 1842. On the distribution of the erratic boulders and on the contemporaneous unstratified deposits of South America. *Transactions of the Geological Society, London, Series* 2, **6**, 415–431, https://doi.org/10.1144/transgslb.6.2.415
- Davies, J.H. and von Blanckenburg, F. 1995. Slab breakoff: a model of lithosphere detachment and its test in the magmatism and deformation of collisional orogens. *Earth and Planetary Science Letters*, 129, 85–102, https:// doi.org/10.1016/0012-821X(94)00237-S
- Dávila, F., Ávila, P. et al. 2019. Measuring dynamic topography in South America. In: Horton, B.K. and Folguera, A. (eds) Andean Tectonics. Elsevier, 35–66, https://doi.org/10.1016/B978-0-12-816009-1.00003-4
- DeCelles, P.G. 1994. Late Cretaceous—Paleocene synorogenic sedimentation and kinematic history of the Sevier thrust belt, northeast Utah and southwest

- Wyoming. GSA Bulletin, 106, 32–56, https://doi.org/10.1130/0016-7606 (1994)106<0032;LCPSSA>2.3.CO;2
- DeCelles, P.G. 2012. Foreland basin systems revisited: variations in response to tectonic settings. In: Busby, C. and Azor, A. (eds) Tectonics of Sedimentary Basins: Recent Advances. Blackwell Publishing, 405–426, https://doi.org/10. 1002/9781444347166.ch20
- DeCelles, P.G. and DeCelles, P.C. 2001. Rates of shortening, propagation, underthrusting, and flexural wave migration in continental orogenic systems. *Geology*, **29**, 135–138, https://doi.org/10.1130/0091-7613(2001)029<0135: ROSPUA>2.0.CO;2
- DeCelles, P.G. and Giles, K.N. 1996. Foreland basin systems. *Basin Research*, **8**, 105–123, https://doi.org/10.1046/j.1365-2117.1996.01491.x
- DeCelles, P.G. and Horton, B.K. 2003. Early to middle Tertiary foreland basin development and the history of Andean crustal shortening in Bolivia. GSA Bulletin, 115, 58–77, https://doi.org/10.1130/0016-7606(2003)115<0058: ETMTFB>2.0.CO;2
- DeCelles, P.G. and Mitra, G. 1995. History of the Sevier orogenic wedge in terms of critical taper models, northeast Utah and southwest Wyoming. *GSA Bulletin*, **107**, 454–462, https://doi.org/10.1130/0016-7606(1995)107<0454: HOTSOW>2.3.CO;2
- DeCelles, P.G., Carrapa, B., Horton, B.K. and Gehrels, G.E. 2011. Cenozoic foreland basin system in the central Andes of northwestern Argentina: implications for Andean geodynamics and modes of deformation. *Tectonics*, 30, TC6013, https://doi.org/10.1029/2011TC002948
- Delgado, A., Mora, A. and Reyes-Harker, A. 2012. Deformation partitioning in the Llanos foreland basin during the Cenozoic and its correlation with mountain building in the hinterland. *Journal of South American Earth Sciences*, 39, 228–244, https://doi.org/10.1016/j.jsames.2012.04.011
- DeMets, C., Gordon, R.G. and Argus, D.F. 2010. Geologically current plate motions. *Geophysical Journal International*, **181**, 1–80, https://doi.org/10.1111/j.1365-246X.2009.04491.x
- de Vicente, G., Cloetingh, S., Van Wees, J.D. and Cunha, P.P. 2011. Tectonic classification of Cenozoic Iberian foreland basins. *Tectonophysics*, 502, 38–61, https://doi.org/10.1016/j.tecto.2011.02.007
- Dewey, J.F. 1980. Episodicity, sequence and style at convergent plate boundaries. Geological Association of Canada, Special Papers, 20, 553–573.
- Dewey, J.F. and Bird, J.M. 1970. Mountain belts and the new global tectonics. Journal of Geophysical Research, 75, 2625–2647, https://doi.org/10.1029/ JB075i014p02625
- Dickinson, W.R. 1974. Plate tectonics and sedimentation. SEPM Special Publications, 22, 1–27.
- Dickinson, W.R., Klute, M.A., Hayes, M.J., Janecke, S.U., Lundin, E.R., McKittrick, M.A. and Olivares, M.D. 1988. Paleogeographic and paletotectonic setting of Laramide sedimentary basins in the central Rocky-Mountain region. GSA Bulletin, 100, 1023–1039, https://doi.org/10.1130/0016-7606 (1988)100<1023:PAPSOL>2.3.CO;2
- Dickinson, W.R., Soreghan, G.S. and Giles, K.A. 1994. Glacio-eustatic origin of Permo-Carboniferous stratigraphic cycles: evidence from the southern Cordilleran foreland region. SEPM, Concepts in Sedimentology and Paleontology, 4, 25–34.
- Duarte, E., Bayona, G., Jaramillo, C., Parra, M., Romero, I. and Mora, J.A. 2017. Identificación de los máximos eventos de inundación marina miocenos y su uso en la correlación y análisis de la cuenca de antepaís de los Llanos orientales, Colombia. *Boletín de Geología*, 39, 19–40, https://doi.org/10.18273/revbol.v39n1-2017001
- Dumont, J.F. 1996. Neotectonics of the Subandes-Brazilian craton boundary using geomorphological data: the Marañon and Beni basins. *Tectonophysics*, 259, 137–151, https://doi.org/10.1016/0040-1951(95)00200-6
- Echavarria, L., Hernández, R., Allmendinger, R. and Reynolds, J. 2003. Subandean thrust and fold belt of northwestern Argentina: geometry and timing of the Andean evolution. AAPG Bulletin, 87, 965–985, https://doi.org/ 10.1306/01200300196
- Erslev, E.A. 2005. 2D Laramide geometries and kinematics of the Rocky Mountains, western U.S.A. American Geophysical Union, Geophysical Monographs, 154, 7–20, https://doi.org/10.1029/154GM0
- Espurt, N., Baby, P. et al. 2007. How does the Nazca Ridge subduction influence the modern Amazonian foreland basin? Geology, 35, 515–518, https://doi.org/ 10.1130/G23237A.1
- Espurt, N., Baby, P., Brusset, S., Roddaz, M., Hermoza, W. and Barbarand, J. 2010. The Nazca Ridge and uplift of the Fitzcarrald Arch: implications for regional geology in northern South America. *In*: Hoorn, C. and Wesselingh, F.P. (eds) *Amazonia: Landscape and Species Evolution: A Look into the Past*. Wiley-Blackwell, 38–60, https://doi.org/10.1002/9781444306408.ch6
- Espurt, N., Barbarand, J., Roddaz, M., Brusset, S., Baby, P., Saillard, M. and Hermoza, W. 2011. A scenario for late Neogene Andean shortening transfer in the Camisea Subandean zone (Peru, 12°S): implications for growth of the northern Andean Plateau. GSA Bulletin, 123, 2050–2068, https://doi.org/10. 1130/B30165.1
- Ettensohn, F.R. 1994. Tectonic control on formation and cyclicity of major Appalachian unconformities and associated stratigraphic sequences. SEPM, Concepts in Sedimentology and Paleontology, 4, 217–242.
- Faccenna, C. and Becker, T.W. 2020. Topographic expressions of mantle dynamics in the Mediterranean. *Earth-Science Reviews*, 209, 103327, https://doi.org/10. 1016/j.earscirev.2020.103327

- Fernández Paz, L., Bechis, F. *et al.* 2019. Constraints on trenchward migration and back-arc magmatism in the North Patagonian Andes in the context of Nazca plate rollback. *Tectonics*, **38**, 3794–3817, https://doi.org/10.1029/2019TC005580
- Feruglio, E. 1950. Descripción Geológica de la Patagonia. Yacimientos Petrolíferos Fiscales, Buenos Aires.
- Fitch, T.J. 1972. Plate convergence, transcurrent faults, and internal deformation adjacent to Southeast Asia and the western Pacific. *Journal of Geophysical Research*, 77, 4432–4460, https://doi.org/10.1029/JB077i023p04432
- Flament, N., Gurnis, M., Müller, R.D., Bower, D.J. and Husson, L. 2015. Influence of subduction history on South American topography. *Earth and Planetary Science Letters*, 430, 9–18, https://doi.org/10.1016/j.epsl.2015.08.006
- Flemings, P.B. and Jordan, T.E. 1989. A synthetic stratigraphic model of foreland basin development. *Journal of Geophysical Research*, **94**, 3851–3866, https://doi.org/10.1029/JB094iB04p03851
- Flemings, P.B. and Jordan, T.E. 1990. Stratigraphic modeling of foreland basins: interpreting thrust deformation and lithosphere rheology. *Geology*, **18**, 430–434, https://doi.org/10.1130/0091-7613(1990)018<0430:SMOFBI>2.3.CO;2
- Folguera, A., Rojas Vera, E., Bottessi, G., Zamora Valcarce, G. and Ramos, V.A. 2010. The Loncopué trough: a Cenozoic basin produced by extension in the southern Central Andes. *Journal of Geodynamics*, 49, 287–295, https://doi. org/10.1016/j.jog.2010.01.009
- Folguera, A., Gianni, G. et al. 2015a. A review about the mechanisms associated with active deformation, regional uplift and subsidence in southern South America. Journal of South American Earth Sciences, 64, 511–529, https://doi. org/10.1016/j.jsames.2015.07.007
- Folguera, A., Bottesi, G. *et al.* 2015*b*. Exhumation of the Neuquén Basin in the southern Central Andes (Malargüe fold and thrust belt) from field data and low-temperature thermochronology. *Journal of South American Earth Sciences*, **64**, 381–398, https://doi.org/10.1016/j.jsames.2015.08.003
- Folguera, A., Zárate, M., Tedesco, A., Dávila, F. and Ramos, V.A. 2015c. Evolution of the Neogene Andean foreland basins of the southern Pampas and northern Patagonia (34°–41°S), Argentina. *Journal of South American Earth Sciences*, **64**, 452–466, https://doi.org/10.1016/j.jsames.2015.05.010
- Fosdick, J.C., Romans, B.W., Fildani, A., Bernhardt, A., Calderón, M. and Graham, S.A. 2011. Kinematic evolution of the Patagonian retroarc fold-and-thrust belt and Magallanes foreland basin, Chile and Argentina, 51°30′S. *GSA Bulletin*, **123**, 1679–1698, https://doi.org/10.1130/b30242.1
- Fosdick, J.C., Graham, S.A. and Hilley, G.E. 2014. Influence of attenuated lithosphere and sediment loading on flexure of the deep-water Magallanes retroarc foreland basin, southern Andes. *Tectonics*, **33**, 2505–2525, https://doi.org/10.1002/2014TC003684
- Fosdick, J.C., Grove, M., Graham, S.A., Hourigan, J.K., Loveras, O. and Romans, B.W. 2015. Detrital thermochronologic record of burial heating and sediment recycling in the Magallanes foreland basin, Patagonian Andes. Basin Research, 27, 546–572, https://doi.org/10.1111/bre.12088
 Fosdick, J.C., VanderLeest, R.V., Bostelmann, J.E., Leonard, J.S., Ugalde, R.,
- Fosdick, J.C., VanderLeest, R.V., Bostelmann, J.E., Leonard, J.S., Ugalde, R., Oyarzún, J.L. and Griffin, M. 2020. Revised timing of Cenozoic Atlantic incursions and changing hinterland sediment sources during southern Patagonian orogenesis. *Lithosphere*, 2020, 8883099, https://doi.org/10.2113/ 2020/8883099
- Fuentes, F. and Horton, B.K. 2020. The Andean foreland evolution of the Neuquén Basin: a discussion. In: Kietzmann, D. and Folguera, A. (eds) Opening and Closure of the Neuquén Basin in the Southern Andes. Springer, 341–370, https://doi.org/10.1007/978-3-030-29680-3_14
- Fuentes, F., DeCelles, P.G. and Gehrels, G.E. 2009. Jurassic onset of foreland basin deposition in northwestern Montana, USA: implications for along-strike synchroneity of Cordilleran orogenic activity. *Geology*, 37, 379–382, https://doi. org/10.1130/G25557A.1
- Fuentes, F., Horton, B.K., Starck, D. and Boll, A. 2016. Structure and tectonic evolution of hybrid thick- and thin-skinned systems in the Malargüe fold– thrust belt, Neuquén basin, Argentina. *Geological Magazine*, 153, 1066–1084, https://doi.org/10.1017/S0016756816000583
- Garrido, A., Kramarz, A., Forasiepi, A. and Bond, M. 2012. Estratigrafia, mamíferos fósiles y edad de las secuencias volcanosedimentarias eocenomiocenas de la sierra de Huantraico-sierra Negra y cerro Villegas (provincia del Neuquén, Argentina). Andean Geology, 39, 482–510.
- Garzione, C.N., McQuarrie, N. et al. 2017. The tectonic evolution of the Central Andean Plateau and geodynamic implications for the growth of plateaus. Annual Review of Earth and Planetary Sciences, 45, 529–559, https://doi.org/10.1146/annurey-earth-063016-020612
- George, S.W.M., Davis, S.N., Fernández, R.A., Manríquez, L.M.E., Leppe, M.A., Horton, B.K. and Clarke, J.A. 2020. Chronology of deposition and unconformity development across the Cretaceous–Paleogene boundary, Magallanes-Austral Basin, Patagonian Andes. *Journal of South American Earth Sciences*, 97, https://doi.org/10.1016/j.jsames.2019.102237
 Ghiglione, M.C. and Ramos, V.A. 2005. Progression of deformation and
- Ghiglione, M.C. and Ramos, V.A. 2005. Progression of deformation and sedimentation in the southernmost Andes. *Tectonophysics*, 405, 25–46, https:// doi.org/10.1016/j.tecto.2005.05.004
- Ghiglione, M.C., Ramos, V.A. and Cristallini, E.O. 2002. Fueguian Andes foreland fold and thrust belt: structure and growth strata. Revista Geológica de Chile, 29, 17–41, https://doi.org/10.4067/S0716-02082002000100002
- Ghiglione, M.C., Quinteros, J. et al. 2010. Structure and tectonic history of the foreland basins of southernmost South America. *Journal of South American* Earth Sciences, 29, 262–277, https://doi.org/10.1016/j.jsames.2009.07.006

Ghiglione, M.C., Likerman, J., Giambiagi, L.B., Aguirre-Urreta, B. and Suarez, F. 2014. Geodynamic context for the deposition of coarse-grained deep-water axial channel systems in the Patagonian Andes. *Basin Research*, 26, 726–745, https://doi.org/10.1111/bre.12061

- Ghiglione, M.C., Ramos, V., Cuitiño, J. and Barberón, V. 2016a. Growth of the southern Patagonian Andes (46–53°S) and its relation with subduction processes. *In:* Folguera, A., Naipauer, M., Sagripanti, L., Ghiglione, M.C., Orts, D.L. and Giambiagi, L. (eds) *Growth of the Southern Andes*. Springer, 201–240.
- Ghiglione, M.C., Sue, C., Ramos, M.E., Tobal, J.E. and Gallardo, R.E. 2016b. The relation between Neogene denudation of the southernmost Andes and sedimentation in the offshore Argentine and Malvinas basins during the opening of the Drake Passage. *In*: Ghiglione, M. (ed.) *Geodynamic Evolution of the Southernmost Andes: Connections with the Scotia Arc.* Springer, 109–135.
- Ghiglione, M.C., Ronda, G. et al. 2019. Structure and tectonic evolution of the South Patagonian fold and thrust belt: coupling between subduction dynamics, climate and tectonic deformation. In: Horton, B.K. and Folguera, A. (eds) Andean Tectonics. Elsevier, 675–697, https://doi.org/10.1016/B978-0-12-816009-1.00024-1
- Giambiagi, L.B., Tunik, M.A. and Ghiglione, M. 2001. Cenozoic tectonic evolution of the Alto Tunuyán foreland basin above the transition zone between the flat and normal subduction segments (33°30′–34°S), western Argentina. *Journal of South American Earth Sciences*, 14, 707–724, https://doi.org/10.1016/S0895-9811(01)00059-1
- Giambiagi, L., Bechis, F., Garcia, V. and Clark, A.H. 2008. Temporal and spatial relationships of thick- and thin-skinned deformation: a case study from the Malargüe fold and thrust belt, southern Central Andes. *Tectonophysics*, **459**, 123–139, https://doi.org/10.1016/j.tecto.2007.11.069
- Giambiagi, L., Mescua, J., Bechis, F., Tassara, A. and Hoke, G.D. 2012. Thrust belts of the southern Central Andes: along-strike variations in shortening, topography, crustal geometry, and denudation. GSA Bulletin, 124, 1339–1351, https://doi.org/10.1130/B30609.1
- Gianni, G.M., Dávila, F. et al. 2018. A geodynamic model linking Cretaceous orogeny, are migration, foreland basin subsidence and marine ingression in southern South America. Earth Science Reviews, 185, 437–462, https://doi. org/10.1016/j.earscirev.2018.06.016
- Gianni, G.M., Navarrete, C. and Spagnotto, S. 2019. Surface and mantle records reveal an ancient slab tear beneath Gondwana. *Scientific Reports*, 9, 19774, https://doi.org/10.1038/s41598-019-56335-9
- Gillis, R.J., Horton, B.K. and Grove, M. 2006. Thermochronology, geochronology, and upper crustal structure of the Cordillera Real: implications for Cenozoic exhumation of the central Andean plateau. *Tectonics*, 25, TC6007, https://doi.org/10.1029/2005TC001887
- Giovanni, M.K., Horton, B.K., Garzione, C.N., McNulty, B. and Grove, M. 2010. Extensional basin evolution in the Cordillera Blanca, Peru: stratigraphic and isotopic records of detachment faulting and orogenic collapse in the Andean hinterland. *Tectonics*, 29, TC6007, https://doi.org/10.1029/2010TC002666
- Gómez, E., Jordan, T.E., Allmendinger, R.W. and Cardozo, N. 2005. Development of the Colombian foreland-basin system as a consequence of diachronous exhumation of the northern Andes. GSA Bulletin, 117, 1272–1292, https://doi.org/10.1130/B25456.1
- Gorroño, R., Pascual, R. and Pombo, R. 1979. Hallazgo de mamíferos eógenos en el sur de Mendoza. Su implicancia en las dataciones de los 'Rodados Lustrosos' y del primer episodio orogénico del Terciario en esa region. In: Asociación Geológica Argentina (ed.) VII Congreso Geológico Argentino, Actas II, Neuquén, 475–487.
- Guillaume, B., Martinod, J., Husson, L., Roddaz, M. and Riquelme, R. 2009. Neogene uplift of central eastern Patagonia: dynamic response to active spreading ridge subduction? *Tectonics*, 28, TC2009, https://doi.org/10.1029/ 2008TC002324
- Guillaume, B., Gautheron, C., Simon-Labric, T., Martinod, J., Roddaz, M. and Douville, E. 2013. Dynamic topography control on Patagonian relief evolution as inferred from low temperature thermochronology. *Earth and Planetary Science Letters*, 364, 157–167, https://doi.org/10.1016/j.epsl.2012.12.036
- Gupta, S. and Allen, P.A. 2000. Implications of foreland paleotopography for stratigraphic development in the Eocene distal Alpine foreland basin. GSA Bulletin, 112, 515–530, https://doi.org/10.1130/0016-7606(2000)112<515: IOFPES>2.0.CO:2
- Gutscher, M.A., Spakman, W., Bijwaard, H. and Engdahl, E.R. 2000. Geodynamics of flat subduction: seismicity and tomographic constraints from the Andean margin. *Tectonics*, 19, 814–833, https://doi.org/10.1029/ 1000TC001152
- Hampel, A. 2002. The migration history of the Nazca Ridge along the Peruvian active margin: a re-evaluation. *Earth and Planetary Science Letters*, **203**, 665–679, https://doi.org/10.1016/S0012-821X(02)00859-2
- Heidbach, O., Rajabi, M. et al. 2018. The World Stress Map database release 2016: crustal stress pattern across scales. Tectonophysics, 744, 484–498, https://doi.org/10.1016/j.tecto.2018.07.007
- Heller, P.L., Angevine, C.L., Winslow, N.S. and Paola, C. 1988. Two-phase stratigraphic model of foreland-basin sequences. *Geology*, 16, 501–504, https://doi.org/10.1130/0091-7613(1988)016<0501:TPSMOF>2.3.CO;2
- Horton, B. K. 1999. Erosional control on the geometry and kinematics of thrust belt development in the central Andes. *Tectonics*, 18, 1292–1304, https://doi. org/10.1029/1999TC900051

- Horton, B.K. 2005. Revised deformation history of the central Andes: inferences from Cenozoic foredeep and intermontane basins of the Eastern Cordillera, Bolivia. *Tectonics*, 24, TC3011, https://doi.org/10.1029/2003TC001619
- Horton, B.K. 2012. Cenozoic evolution of hinterland basins in the Andes and Tibet. In: Busby, C. and Azor, A. (eds) Tectonics of Sedimentary Basins: Recent Advances. Blackwell Publishing, 427–444, https://doi.org/10.1002/ 9781444347166.ch21
- Horton, B.K. 2018a. Sedimentary record of Andean mountain building. Earth Science Reviews, 178, 279–309, https://doi.org/10.1016/j.earscirev.2017.11.025
- Horton, B.K. 2018b. Tectonic regimes of the central and southern Andes: responses to variations in plate coupling during subduction. *Tectonics*, 37, 402–429, https://doi.org/10.1002/2017TC004624
- Horton, B.K. and DeCelles, P.G. 1997. The modern foreland basin system adjacent to the central Andes. Geology, 25, 895–898, https://doi.org/10.1130/ 0091-7613(1997)025<0895:TMFBSA>2.3.CO;2
- Horton, B.K. and DeCelles, P.G. 2001. Modern and ancient fluvial megafans in the foreland basin system of the central Andes, southern Bolivia: implications for drainage network evolution in fold–thrust belts. *Basin Research*, **13**, 43–63, https://doi.org/10.1046/j.1365-2117.2001.00137.x
- Horton, B.K. and Fuentes, F. 2016. Sedimentary record of plate coupling and decoupling during growth of the Andes. *Geology*, 44, 647–650, https://doi. org/10.1130/G37918.1
- Horton, B.K., Saylor, J.E., Nie, J., Mora, A., Parra, M., Reyes-Harker, A. and Stockli, D.F. 2010. Linking sedimentation in the northern Andes to basement configuration, Mesozoic extension, and Cenozoic shortening: evidence from detrital zircon U–Pb ages, Eastern Cordillera, Colombia. GSA Bulletin, 122, 1423–1442, https://doi.org/10.1130/B30118.1
- Horton, B.K., Perez, N.D., Fitch, J.D. and Saylor, J.E. 2015. Punctuated shortening and subsidence in the Altiplano plateau of southern Peru: implications for early Andean mountain building. *Lithosphere*, 7, 117–137, https://doi.org/10.1130/L397.1
- Horton, B.K., Fuentes, F., Boll, A., Starck, D., Ramirez, S.G. and Stockli, D.F. 2016. Andean stratigraphic record of the transition from backarc extension to orogenic shortening: a case study from the northern Neuquén basin, Argentina. *Journal of South American Earth Sciences*, 71, 17–40, https://doi.org/10.1016/j.jsames.2016.06.003
- Horton, B.K., Parra, M. and Mora, A. 2020. Construction of the Eastern Cordillera of Colombia: insights from the sedimentary record. *In*: Gómez, J. and Mateus-Zabala, D. (eds) *The Geology of Colombia*. Vol. 37. Servicio Geológico Colombiano, Publicaciones Geológicas Especiales, Bogotá, 67–88, https://doi.org/10.32685/pub.esp.37.2019.03
- Houston, W.S., Huntoon, J.E. and Kamola, D.L. 2000. Modeling of Cretaceous foreland-basin parasequences, Utah, with implications for timing of Sevier thrusting. *Geology*, 28, 267–270, https://doi.org/10.1130/0091-7613(2000) 28<267:MOCFPU>2.0.CO;2
- Iribarne, M., Callot, P. et al. 2018. Stratigraphy, structural styles, and hydrocarbon potential of the Ene Basin: an exploration opportunity in the sub-Andean fold-and-thrust belt of Peru. AAPG Memoirs, 117, 293–318, https://doi.org/10.1306/13622125M1173771
- Jaillard, E. and Soler, P. 1996. Cretaceous to Paleogene tectonic evolution of the northern Central Andes (0–18°S) and its relations to geodynamics. *Tectonophysics*, 259, 41–53, https://doi.org/10.1016/0040-1951(95)00107-7
- James, D.E. and Sacks, S. 1999. Cenozoic formation of the central Andes: a geophysical perspective. Society of Economic Geologists, Special Publications, 7, 1–25.
- Jaramillo, C., Romero, I. et al. 2017. Miocene flooding events of western Amazonia. Science Advances, 3, https://doi.org/10.1126/sciadv.1601693
- Jarrard, R.D. 1986. Relations among subduction parameters. Reviews of Geophysics, 24, 217–284, https://doi.org/10.1029/RG024i002p00217
- Jordan, T.E. 1981. Thrust loads and foreland basin evolution, Cretaceous, western United States. AAPG Bulletin, 65, 2506–2520.
- Jordan, T.E. 1995. Retroarc foreland and related basins. In: Busby, C.J. and Ingersoll, R.V. (eds) Tectonics of Sedimentary Basins. Blackwell Science, 331–362.
- Jordan, T.E. and Alonso, R.N. 1987. Cenozoic stratigraphy and basin tectonics of the Andes Mountains, 20°–28° south latitude. AAPG Bulletin, 71, 49–64.
- Jordan, T.E. and Flemings, P.B. 1991. Large-scale stratigraphic architecture, eustatic variation, and unsteady tectonism: a theoretical evaluation. Journal of Geophysical Research, 96, 6681–6899, https://doi.org/10.1029/901801399
- Jordan, T.E., Isacks, B.L., Allmendinger, R.W., Brewer, J.A., Ramos, V.A. and Ando, C.J. 1983. Andean tectonics related to geometry of subducted Nazca plate. GSA Bulletin, 94, 341–361, https://doi.org/10.1130/0016-7606(1983) 94<341:ATRTGO>2.0.CO;2
- Jordan, T.E., Allmendinger, R.W., Damanti, J.F. and Drake, R. E. 1993. Chronology of motion in a complete thrust belt: the Precordillera, 30–31°S, Andes Mountains. *Journal of Geology*, 101, 135–156, https://doi.org/10. 1006/48913
- Jordan, T.E., Schlunegger, F. and Cardozo, N. 2001a. Unsteady and spatially variable evolution of the Neogene Andean Bermejo foreland basin, Argentina. *Journal of South American Earth Sciences*, 14, 775–798, https://doi.org/10. 1016/S0895-9811(01)00072-4
- Jordan, T.E., Burns, W.M., Veiga, R., Pángaro, F., Copeland, P., Kelley, S. and Mpodozis, C. 2001b. Extension and basin formation in the southern Andes caused by increased convergence rate: a mid-Cenozoic trigger for the Andes. *Tectonics*, 20, 308–324, https://doi.org/10.1029/1999TC001181

- Jutras, P., Young, G.M. and Caldwell, W.G.E. 2011. Reinterpretation of James Hutton's historic discovery on the Isle of Arran as a double unconformity masked by a phreatic calcrete hardpan. *Geology*, 39, 147–150, https://doi.org/ 10.1130/G31490.1
- Kley, J. and Voigt, T. 2008. Late Cretaceous intraplate thrusting in central Europe: effect of Africa–Iberia–Europe convergence, not Alpine collision. *Geology*, 36, 839–842, https://doi.org/10.1130/G24930A.1
- Kley, J., Monaldi, C.R. and Salfity, J.A. 1999. Along-strike segmentation of the Andean foreland: causes and consequences. *Tectonophysics*, 301, 75–94, https://doi.org/10.1016/S0040-1951(98)90223-2
- Lacombe, O. and Bellahsen, N. 2016. Thick-skinned tectonics and basement-involved fold-thrust belts: insights from selected Cenozoic orogens. *Geological Magazine*, 152, 763–810, https://doi.org/10.1017/S0016756816000078
- Lagabrielle, Y., Suárez, M., Rossello, E.A., Hérail, G., Martinod, J., Régnier, M. and de la Cruz, R. 2004. Neogene to Quaternary tectonic evolution of the Patagonian Andes at the latitude of the Chile triple junction. *Tectonophysics*, 385, 211–241, https://doi.org/10.1016/j.tecto.2004.04.023
- Lalami, H.R.K., Hajialibeigi, H., Sherkati, S. and Adabi, M.H. 2020. Tectonic evolution of the Zagros foreland basin since Early Cretaceous, SW Iran: regional tectonic implications from subsidence analysis. *Journal of Asian Earth Sciences*, 204, 104550, https://doi.org/10.1016/j.jseaes.2020.104550
- Lawton, T.F. 2019. Laramide sedimentary basins and sediment-dispersal systems. In: Miall, A.D. (ed.) The Sedimentary Basins of the United States and Canada. Elsevier, 529–557, https://doi.org/10.1016/B978-0-444-63895-3.00013-9
- Legarreta, L. and Uliana, M.A. 1991. Jurassic-Cretaceous marine oscillations and geometry of back-arc basin fill, central Argentine Andes. *International Association of Sedimentologists, Special Publications*, 12, 429-450.
- Liu, S., Nummedal, D. and Liu, L. 2011. Migration of dynamic subsidence across the Late Cretaceous United States Western Interior Basin in response to Farallon plate subduction. *Geology*, 39, 555–558, https://doi.org/10.1130/ G31692.1
- Londono, J., Lorenzo, J.M. and Ramirez, V. 2012. Lithospheric flexure and related base-level stratigraphic cycles in continental foreland basins: an example from the Putumayo Basin, Northern Andes. AAPG Memoirs, 100, 357–375, https://doi.org/10.1306/13351561M1003537
- Lonsdale, P. 2005. Creation of the Cocos and Nazca plates by fission of the Farallon plate. *Tectonophysics*, 404, 237–264, https://doi.org/10.1016/j.tecto. 2005.05.011
- Loutit, T.S., Hardenbol, J., Vail, P.R. and Baum, G.R. 1988. Condensed sections: the key to age dating and correlation of continental margin sequences. SEPM Special Publications, 42, 183–213.
- Maloney, K.T., Clarke, G.L., Klepeis, K.A. and Quevedo, L. 2013. The Late Jurassic to present evolution of the Andean margin: drivers and the geological record. *Tectonics*, 32, 1049–1065, https://doi.org/10.1002/tect.20067
- Malumián, N. 2002. El Terciario marino: Sus relaciones con el eustatismo. In: Haller, M.J. (ed.) Geología y Recursos Naturales de Santa Cruz. XV Congreso Geológico Argentino, Relatorio, Buenos Aires, 237–244.
- Malumián, N., Panza, J.L., Parisi, C., Nañez, C., Carames, A. and Torre, A. 2000.Hoja Geológica 5172-III-Yaciento Río Turbio, provincia Santa Cruz, 1:250.000. Servicio Geológico Minero Argentino, Boletin, 247.
- Mamani, M., Wörner, G. and Sempere, T. 2010. Geochemical variations in igneous rocks of the central Andean orocline (13°S to 18°S): tracing crustal thickening and magma generation through time and space. GSA Bulletin, 122, 162–182, https://doi.org/10.1130/B26538.1
- Manceda, R. and Figueroa, D. 1995. Inversion of the Mesozoic Neuquén rift in the Malargüe fold and thrust belt, Mendoza, Argentina. AAPG Memoirs, 62, 369–382.
- Martínez, O.A., Rabassa, J. and Coronato, A. 2009. Charles Darwin and the first scientific observations on the Patagonian Shingle Formation (Rodados Patagónicos). Revista de la Asociación Geológica Argentina, 64, 90–100.
- Martinod, J., Husson, L., Roperch, P., Guillaume, B. and Espurt, N. 2010. Horizontal subduction zones, convergence velocity and the building of the Andes. *Earth and Planetary Science Letters*, 299, 299–309, https://doi.org/10. 1016/j.epsl.2010.09.010
- McQuarrie, N. 2002. The kinematic history of the central Andean fold–thrust belt, Bolivia: implications for building a high plateau. GSA Bulletin, 114, 950–963, https://doi.org/10.1130/0016-7606(2002)114<0950:TKHOTC>2.0.CO;2
- McQuarrie, N. and Chase C.G. 2000. Raising the Colorado Plateau. *Geology*, **28**, 91–94, https://doi.org/10.1130/0091-7613(2000)028<0091:RTCP>2.0.CO;2
- McQuarrie, N., Horton, B.K., Zandt, G., Beck, S. and DeCelles, P.G. 2005. Lithospheric evolution of the Andean fold–thrust belt, Bolivia, and the origin of the central Andean plateau. *Tectonophysics*, 399, 15–37, https://doi.org/10. 1016/j.tecto.2004.12.013
- McQueen, H.W.S. and Beaumont, C. 1989. Mechanical models of tilted block basins. American Geophysical Union, Geophysical Monographs, 48, 65–71.
- Mégard, F., Noble, D.C., McKee, E.H. and Bellon, H. 1984. Multiple pulses of Neogene compressive deformation in the Ayacucho intermontane basin, Andes of central Peru. GSA Bulletin, 95, 1108–1117, https://doi.org/10.1130/ 0016-7606(1984)95<1108:MPONCD>2.0.CO;2
- Miall, A. 1996. The Geology of Stratigraphic Sequences. Springer.
- Miall, A.D. 2016. The valuation of unconformities. *Earth-Science Reviews*, **163**, 22–71, https://doi.org/10.1016/j.earscirev.2016.09.011
- Mitrovica, J.X., Beaumont, C. and Jarvis, G.T. 1989. Tilting of continental interiors by the dynamical effects of subduction. *Tectonics*, 8, 1079–1094, https://doi.org/10.1029/TC008i005p01079

- Montero-López, C., del Papa, C., Hongn, F., Strecker, M. and Aramayo, A. 2018. Synsedimentary broken-foreland tectonics during the Paleogene in the Andes of NW Argentine: new evidence from regional to centimeter-scale deformation features. *Basin Research*, 30, 142–159, https://doi.org/10.1111/ bre.12212
- Montgomery, D.R., Balco, G. and Willett, S.D. 2001. Climate, tectonics, and the morphology of the Andes. *Geology*, **29**, 579–582, https://doi.org/10.1130/ 0091-7613(2001)029<0579:CTATMO>2.0.CO;2
- Mora, A., Parra, M., Strecker, M.R., Sobel, E.R., Hooghiemstra, H., Torres, V. and Jaramillo, J.V. 2008. Climatic forcing of asymmetric orogenic evolution in the Eastern Cordillera of Colombia. GSA Bulletin, 120, 930–949, https://doi.org/10.1130/B26186.1
- Mora, A., Baby, P., Roddaz, M., Parra, M., Brusset, S., Hermoza, W. and Espurt, N. 2010. Tectonic history of the Andes and sub-Andean zones: implications for the development of the Amazon drainage basin. *In:* Hoom, C. and Wesselingh, F.P. (eds) *Amazonia: Landscape and Species Evolution: A Look Into the Past.* Wiley-Blackwell, 38–60, https://doi.org/10.1002/9781444306408.ch4
- Mora, A., Reyes-Harker, A. et al. 2013. Inversion tectonics under increasing rates of shortening and sedimentation: Cenozoic example from the Eastern Cordillera of Colombia. Geological Society, London, Special Publications, 377, 411–442, https://doi.org/10.1144/SP377.6
- Morin, J., Jolivet, M., Barrier, L., Laborde, A., Li, H. and Dauteuil, O. 2019. Planation surfaces of the Tian Shan Range (Central Asia): insight on several 100 million years of topographic evolution. *Journal of Asian Earth Sciences*, 177, 52–65, https://doi.org/10.1016/j.jseaes.2019.03.011
- Mouthereau, F., Filleaudeau, P.Y. *et al.* 2014. Placing limits to shortening evolution in the Pyrenees: role of margin architecture and implications for the Iberia/Europe convergence. *Tectonics*, **33**, 2283–2314, https://doi.org/10.1002/2014TC003663
- Mpodozis, C. and Cornejo, P. 2012. Cenozoic tectonics and porphyry copper systems of the Chilean Andes. Society of Economic Geologists, Special Publications, 16, 329–360.
- Noblet, C., Lavenu, A. and Marocco, R. 1996. Concept of continuum as opposed to periodic tectonism in the Andes. *Tectonophysics*, 255, 65–78, https://doi. org/10.1016/0040-1951(95)00081-X
- Oldow, J.S., Bally, A.W., Avé Lallemant, H.G. and Leeman, W.P. 1989. Phanerozoic evolution of the North American Cordillera; United States and Canada. In: Bally, A.W. and Palmer, A.R. (eds) The Geology of North America—An Overview. The Geology of North America, A. GSA, 139–232.
- Olivero, E.B. and Malumián, N. 2008. Mesozoic–Cenozoic stratigraphy of the Fuegian Andes, Argentina. *Geologica Acta*, **6**, 5–18.
- Pardo-Casas, F. and Molnar, P. 1987. Relative motion of the Nazca (Farallon) and South American plates since late Cretaceous time. *Tectonics*, 6, 233–248, https://doi.org/10.1029/TC006i003p00233
- Parra, M., Mora, A. et al. 2009. Orogenic wedge advance in the northern Andes: evidence from the Oligocene–Miocene sedimentary record of the Medina Basin, Eastern Cordillera, Colombia. GSA Bulletin, 121, 780–800, https://doi.org/10.1130/B26257.1
- Parra, M., Mora, A., Jaramillo, C., Torres, V., Zeilinger, G. and Strecker, M.R. 2010. Tectonic controls on Cenozoic foreland basin development in the north-eastern Andes, Colombia. *Basin Research*, 22, 874–903, https://doi.org/10.1111/j.1365-2117.2009.00459.x
- Parras, A., Griffin, M., Feldmann, R., Casadío, S., Schweitzer, C. and Marenssi, S. 2008. Correlation of marine beds based on Sr- and Ar-date determinations and faunal affinities across the Paleogene/Neogene boundary in southern Patagonia, Argentina. *Journal of South American Earth Sciences*, 26, 204–216, https://doi.org/10.1016/j.jsames.2008.03.006
- Payrola, P., del Papa, C. et al. 2020. Episodic out-of-sequence deformation promoted by Cenozoic fault reactivation in NW Argentina. *Tectonophysics*, 776. https://doi.org/10.1016/j.tecto.2019.228276
- 776, https://doi.org/10.1016/j.tecto.2019.228276
 Pedoja, K., Husson, L., Regard, V., Cobbold, P.R., Ostanciaux, E., Johnson, M.E. and Weill, P. 2011. Relative sea-level fall since the last interglacial stage: are coasts uplifting worldwide? *Earth Science Reviews*, 108, 1–15, https://doi.org/10.1016/j.earscirev.2011.05.002
- Perez, N.D. and Horton, B.K. 2014. Oligocene–Miocene deformational and depositional history of the Andean hinterland basin in the northern Altiplano plateau, southern Peru. *Tectonics*, 33, 1819–1847, https://doi.org/10.1002/ 2014TC003647
- Perez, N.D. and Levine, K.G. 2020. Diagnosing an ancient shallow-angle subduction event from Cenozoic depositional and deformational records in the central Andes of southern Peru. Earth and Planetary Science Letters, 541, 116263, https://doi.org/10.1016/j.epsl.2020.116263
- Pilger, R.H.,Jr 1984. Cenozoic plate kinematics, subduction and magmatism: South American Andes. *Journal of the Geological Society, London*, 141, 793–802, https://doi.org/10.1144/gsjgs.141.5.0793
- Plint, A.G., Hart, B.S. and Donaldson, W.S. 1993. Lithospheric flexure as a control on stratal geometry and facies distribution in Upper Cretaceous rocks of the Alberta foreland basin. *Basin Research*, **5**, 69–77, https://doi.org/10.1111/j.1365-2117.1993.tb00058.x
- Plint, A.G., Tyagi, A. et al. 2012. Dynamic relationship between subsidence, sedimentation, and unconformities in mid-Cretaceous, shallow-marine strata of the Western Canada foreland basin: links to Cordilleran tectonics. In: Busby, C. and Azor, A. (eds) Tectonics of Sedimentary Basins: Recent Advances. Blackwell Publishing, 480–507, https://doi.org/10.1002/9781444347166.ch24

Price, R.A. 1973. Large scale gravitational flow of supracrustal rocks, southern Canadian Rockies. *In*: DeJong, K.A. and Scholten, R.A. (eds) *Gravity and Tectonics*. Wiley, 491–502.

- Price, R.A. 1994. Cordilleran tectonics and the evolution of the Western Canada Sedimentary Basin. In: Mossop, G.D. and Shetsen, I. (eds) Geological Atlas of the Western Canada Sedimentary Basin. Canadian Society of Petroleum Geologists and Alberta Research Council, 13–24, https://repositorio.segemar. gov.ar/handle/308849217/2789
- Proyecto Multinacional Andino 2009. Atlas de deformaciones cuaternarias de Los Andes. Servicio Nacional de Geológia y Minería, Publicacion Geológica Multinacional, 7.
- Rahl, J.M., Harbor, D.J., Galli, C.I. and O'Sullivan, P. 2018. Foreland basin record of uplift and exhumation of the Eastern Cordillera, northwest Argentina. *Tectonics*, 37, 4173–4193, https://doi.org/10.1029/2017TC004955
- Rak, A.J., McQuarrie, N. and Ehlers, T.A. 2017. Kinematics, exhumation, and sedimentation of the north central Andes (Bolivia): an integrated thermochronometer and thermokinematic modeling approach. *Tectonics*, 36, 2524–2554, https://doi.org/10.1002/2016TC004440
- Ramos, V.A. 1989. Andean foothills structures in northern Magallanes Basin, Argentina. AAPG Bulletin, 73, 887–903.
- Ramos, V.A. 1999. Plate tectonic setting of the Andean Cordillera. *Episodes*, **22**, 183–190, https://doi.org/10.18814/epiiugs/1999/v22i3/005
- Ramos, V.A. 2005. Seismic ridge subduction and topography: foreland deformation in the Patagonian Andes. *Tectonophysics*, 399, 73–86, https:// doi.org/10.1016/j.tecto.2004.12.016
- Ramos, V.A. 2009. Anatomy and global context of the Andes: main geologic features and the Andean orogenic cycle. GSA Memoirs, 204, 31–65, https:// doi.org/10.1130/2009.1204(02)
- Ramos, V.A. and Folguera, A. 2009. Andean flat-slab subduction through time. Geological Society, London, Special Publications, 327, 31–54, https://doi.org/ 10.1144/SP327.3
- Ramos, V.A. and Folguera, A. 2011. Payenia volcanic province in the Southern Andes: an appraisal of an exceptional Quaternary tectonic setting. *Journal of Volcanology and Geothermal Research*, 201, 53–64, https://doi.org/10.1016/j.jvolgeores.2010.09.008
- Ramos, V.A. and Kay, S.M. 2006. Overview of the tectonic evolution of the southern Central Andes of Mendoza and Neuquén (35°–39°S latitude). *GSA*, *Special Papers*. **407**. 1–17. https://doi.org/10.1130/2006.2407(01)
- Ramos, V.A., Cristallini, E.O. and Perez, D.J. 2002. The Pampean flat-slab of the Central Andes. *Journal of South American Earth Sciences*, 15, 59–78, https://doi.org/10.1016/S0895-9811(02)00006-8
- Räsänen, M., Neller, R., Salo, J. and Jungner, H. 1992. Recent and ancient fluvial deposition systems in the Amazonian foreland basin, Peru. Geological Magazine, 129, 296–306, https://doi.org/10.1017/S0016756800019233
- Regard, V., Lagnous, R. et al. 2009. Geomorphic evidence for recent uplift of the Fitzcarrald Arch (Peru): a response to the Nazca Ridge subduction. Geomorphology, 107, 107–117, https://doi.org/10.1016/j.geomorph.2008.12.
- Reyes-Harker, A., Ruiz-Valdivieso, C.F. et al. 2015. Cenozoic paleogeography of the Andean foreland and retroarc hinterland of Colombia. AAPG Bulletin, 99, 1407–1453, https://doi.org/10.1306/06181411110
- Riba, O. 1976. Syntectonic unconformities of the Alto Cardener, Spanish Pyrenees: a genetic interpretation. Sedimentary Geology, 15, 213–233, https://doi.org/10.1016/0037-0738(76)90017-8
- Roddaz, M., Hermoza, W. et al. 2010. Cenozoic sedimentary evolution of the Amazonian foreland basin system. In: Hoorn, C. and Wesselingh, F.P. (eds) Amazonia: Landscape and Species Evolution: A Look Into the Past. Wiley-Blackwell, 61–88, https://doi.org/10.1002/9781444306408.ch5
- Rojas Vera, E.A., Sellés, D. et al. 2014. The origin of the Loncopué Trough in the retroarc of the Southern Central Andes from field, geophysical and geochemical data. *Tectonophysics*, 637, 1–19, https://doi.org/10.1016/j. tecto.2014.09.012
- Ronda, G., Ghiglione, M.C., Barberón, V., Coutand, I. and Tobal, J. 2019. Mesozoic–Cenozoic evolution of the Southern Patagonian Andes fold and thrust belt (47°–48°S): influence of the Rocas Verdes Basin inversion and onset of Patagonian glaciations. *Tectonophysics*, 765, 83–101, https://doi.org/ 10.1016/j.tecto.2019.05.009
- Rosenbaum, G., Giles, D., Saxon, M., Betts, P.G., Weinberg, R.F. and Duboz, C. 2005. Subduction of the Nazca Ridge and the Inca Plateau: insights into the formation of ore deposits in Peru. Earth and Planetary Science Letters, 239, 18–32, https://doi.org/10.1016/j.epsl.2005.08.003
- Ross, G.M., Patchett, P.J., Hamilton, M., Heaman, L., DeCelles, P.G., Rosenberg, E. and Giovanni, M.K. 2005. Evolution of the Cordilleran orogen (southwestern Alberta, Canada) inferred from detrital mineral geochronology, geochemistry, and Nd isotopes in the foreland basin. GSA Bulletin, 117, 747–763, https://doi.org/10.1130/B25564.1
- Royden, L.H. 1993. Evolution of retreating subduction boundaries formed during continental collision. *Tectonics*, 12, 629–638, https://doi.org/10.1029/ 92TC02641
- Rudolph, K.W., Devlin, W.J. and Carabaugh, J.P. 2015. Upper Cretaceous sequence stratigraphy of the Rock Springs uplift, Wyoming. *The Mountain Geologist*, 52, 13–157.
- Sandeman, H.A., Clark, A.H. and Farrar, E. 1995. An integrated tectonomagmatic model for the evolution of the Southern Peruvian Andes (13–20°S)

- since 55 Ma. International Geology Review, 37, 1039–1073, https://doi.org/10.1080/00206819509465439
- Saylor, J.E., Rudolph, K.W., Sundell, K.E. and van Wijk, J. 2020. Laramide orogenesis driven by Late Cretaceous weakening of the North American lithosphere. *Journal of Geophysical Research*, 125, https://doi.org/10.1029/ 20201B019570
- Sempere, T., Marshall, L.G., Rivano, S. and Godoy, E. 1994. Late Oligocene–early Miocene compressional tectosedimentary episode and associated land-mammal faunas in the Andes of central Chile and adjacent Argentina (32–37°S). *Tectonophysics*, 229, 251–264, https://doi.org/10.1016/0040-1951(94)90032-9
- Sempere, T., Butler, R.F., Richards, D.R., Marshall, L.G., Sharp, W. and Swisher, C.C. 1997. Stratigraphy and chronology of Late Cretaceous–early Paleogene strata in Bolivia and northwest Argentina. *GSA Bulletin*, **109**, 709–727, https://doi.org/10.1130/0016-7606(1997)109<0709:SACOUC>2.3.CO;2
- Shanmugam, G., 1988. Origin, recognition, and importance of erosional unconformities in sedimentary basins. *In:* Kleinspehn, K.L. and Paola, C. (eds) *New Perspectives in Basin Analysis*. Springer, 83–108.
- Sickmann, Z.T., Schwartz, T.M. and Graham, S.A. 2018. Refining stratigraphy and tectonic history using detrital zircon maximum depositional age: an example from the Cerro Fortaleza Formation, Austral Basin, southern Patagonia. Basin Research, 30, 708–729, https://doi.org/10.1111/bre.12272
- Siks, B.C. and Horton, B.K. 2011. Growth and fragmentation of the Andean foreland basin during eastward advance of fold–thrust deformation, Puna plateau and Eastern Cordillera, northern Argentina. *Tectonics*, 30, TC6017, https://doi.org/10.1029/2011TC002944
- Silver, P.G., Russo, R.M. and Lithgow-Bertelloni, C. 1998. Coupling of South America and African plate motion and plate deformation. *Science*, 279, 60–63, https://doi.org/10.1126/science.279.5347.60
- Simony, S. and Carr, S.D. 2011. Cretaceous to Eocene evolution of the southeastern Canadian Cordillera: continuity of Rocky Mountain thrust systems with zones of 'in-sequence' mid-crustal flow. *Journal of Structural Geology*, 23, 1417–1434, https://doi.org/10.1016/j.jsg.2011.06.001
- Sinclair, H.D. 1997. Tectonostratigraphic model for underfilled peripheral foreland basins: an Alpine perspective. GSA Bulletin, 109, 324–346, https:// doi.org/10.1130/0016-7606(1997)109<0324:TMFUPF>2.3.CO;2
- Sinclair, H.D. and Naylor, M. 2012. Foreland basin subsidence driven by topographic growth versus plate subduction. GSA Bulletin, 124, 368–379, https://doi.org/10.1130/B30383.1
- Sinclair, H.D., Coakley, B.J., Allen, P.A. and Watts, A.B. 1991. Simulation of foreland basin stratigraphy using a diffusion model of mountain belt uplift and erosion: an example from the Central Alps, Switzerland. *Tectonics*, 10, 599–620, https://doi.org/10.1029/90TC02507
- Sobel, E.R., Hilley, G.E. and Strecker, M.R. 2003. Formation of internally drained contractional basins by aridity-limited bedrock incision. *Journal of Geophysical Research*, 108, 2344, https://doi.org/10.1029/2002JB001883
- Somoza, R. and Ghidella, M.E. 2012. Late Cretaceous to recent plate motions in western South America revisited. *Earth and Planetary Science Letters*, 331– 332, 152–163, https://doi.org/10.1016/j.epsl.2012.03.003
- Starck, D. 2011. Cretaceous—Paleogene basin of northwest Argentina. VIII Congreso de Exploración y Desarrollo de Hidrocarburos. Simposio Cuencas Argentinas, 8, 407–453.
- Steinmann, G. 1929. Geologie von Perú. Carl Winters Universitatsbuchhandlung, Heidelberg.
- Stevens Goddard, A.L. and Fosdick, J.C. 2019. Multichronometer thermochronologic modeling of migrating spreading ridge subduction in southern Patagonia. *Geology*, 47, 555–558, https://doi.org/10.1130/G46091.1
- Stockmal, G.S., Beaumont, C. and Boutilier, R. 1986. Geodynamic models of convergent margin tectonics: Transition from rifted margin to overthrust belt and consequences for foreland-basin development. AAPG Bulletin, 70, 181–190, https://doi.org/10.1306/94885656-1704-11D7-8645000102C1865D
- Suppe, J., Chou, G.T. and Hook, S.C. 1992. Rates of folding and faulting determined from growth strata. *In*: McClay, K.R. (ed.) *Thrust Tectonics*. Chapman and Hall, 105–122.
- Thomson, S.N., Hervé, F. and Stöckhert, B. 2001. Mesozoic–Cenozoic denudation history of the Patagonian Andes (southern Chile) and its correlation to different subduction processes. *Tectonics*, 20, 693–711, https://doi.org/10.1029/2001TC900013
- Thorkelson, D.J. 1996. Subduction of diverging plates and the principles of slab window formation. *Tectonophysics*, **255**, 47–63, https://doi.org/10.1016/0040-1951(95)00106-9
- Tomkeieff, S.I. 1962. Unconformity—an historical study. *Proceedings of the Geologists' Association*, **73**, 383–417, https://doi.org/10.1016/S0016-7878 (62)80031-5
- Turienzo, M.M. 2010. Structural style of the Malargüe fold-and-thrust belt at the Diamante River area (34°30′–34°50′S) and its linkage with the Cordillera Frontal, Andes of central Argentina. *Journal of South American Earth Sciences*, **29**, 537–556, https://doi.org/10.1016/j.jsames.2009.12.002
- Tweto, O. 1980. Summary of Laramide orogeny in Colorado. *In*: Kent, H.C. and Porter, K.W. (eds) *Colorado Geology*. Rocky Mountain Association of Geologists, Denver, CO, 129–134.
- Uba, C.E., Kley, J., Strecker, M.R. and Schmitt, A.K. 2009. Unsteady evolution of the Bolivian Subandean thrust belt: the role of enhanced erosion and clastic wedge progradation. *Earth and Planetary Science Letters*, 281, 134–146, https://doi.org/10.1016/j.epsl.2009.02.010

Unconformities and geodynamics of foreland basins

- Vail. P.R., Hardenbol, J. and Todd, R.G. 1984. Jurassic unconformities. chronostratigraphy, and sea-level changes from seismic stratigraphy and biostratigraphy. AAPG Memoirs, 36, 129-144.
- Van Wagoner, J.C. 1995. Sequence stratigraphy and marine to nonmarine facies architecture of foreland basin strata, Book Cliffs, Utah, USA. AAPG Memoirs, 64 137-223
- Veloza, G., Styron, R., Taylor, M. and Mora, A. 2012. Open-source archive of active faults for northwest South America. GSA Today, 22, https://doi.org/10. 1130/GSAT-G156A.1
- Wagner, L.S., Jaramillo, J.S., Ramírez-Hoyos, L.F., Monsalve, G., Cardona, A. and Becker, T.W. 2017. Transient slab flattening beneath Colombia. Geophysical Research Letters, 44, https://doi.org/10.1002/2017GL073981
- Waschbusch, P.J. and Royden, L.H. 1992a. Spatial and temporal evolution of foredeep basins: lateral strength variations and inelastic yielding in continental lithosphere. Basin Research, 4, 179-196, https://doi.org/10.1111/j.1365-2117.1992.tb00044.x
- Waschbusch, P.J. and Royden, L.H. 1992b. Episodicity in foredeep basins. Geology, 20, 915–918, https://doi.org/10.1130/0091-7613(1992)020<0915: EIFB>2.3.CO;2
- Weimer, R.J. 1984. Relationship of unconformities, tectonics and sea level changes, Cretaceous Western Interior, U.S.A. AAPG Memoirs, 36, 7-36. Wheeler, H.E. 1958. Time-stratigraphy. AAPG Bulletin, 42, 1047-1063.
- Willett, C.D., Ma, K.F., Brandon, M.T., Hourigan, J.K., Christeleit, E.C.
- and Shuster, D.L. 2020. Transient glacial incision in the Patagonian Andes

- from c. 6 Ma to present. Science Advances, 6, https://doi.org/10.1126/sciadv.
- Wilson, T.J. 1991. Transition from back-arc to foreland basin development in southernmost Andes: stratigraphic record from the Ultima Esperanza District, Chile. GSA Bulletin, 103, 98–111, https://doi.org/10.1130/0016-7606(1991) 103<0098:TFBATF>2.3.CO:2
- Yonkee, W.A. and Weil, A.B. 2015. Tectonic evolution of the Sevier and Laramide belts within the North American Cordillera orogenic system. Earth-Science Reviews, 150, 531-593, https://doi.org/10.1016/j.earscirev.2015.08.
- Young, G.M. and Caldwell, W.G.E. 2009. A new look at an old unconformity: field and geochemical data from James Hutton's original unconformity on the Isle of Arran, Scotland. Proceedings of the Geologists' Association, 120, 65-75, https://doi.org/10.1016/j.pgeola.2009.03.004
- Yrigoyen, M.R. 1993. Los depósitos sinorogénicos terciarios. In: Ramos, V.A. (ed.) Geología y Recursos Naturales de Mendoza. Congreso Geológico Argentino, 12, 123-148.
- Zamora, G. and Gil, W. 2018. The Marañón Basin: tectonic evolution and paleogeography. AAPG Memoirs, 117, 121-143, https://doi.org/10.1306/ 13622132m1173768
- Ziegler, P.A., Bertotti, G. and Cloetingh, S. 2002. Dynamic processes controlling foreland development—the role of mechanical (de)coupling of orogenic wedges and forelands. European Geosciences Union, Stephan Mueller Special Publication Series, 1, 17-56.